Rivista Italiana di Paleontologia e Stratigrafia
(*Research in Paleontology and Stratigraphy*)
vol. 131(3): 603-629. **November 2025**
DOI: https://doi.org/10.54103/2039-4942/29039

THE DEEP-SEA HATCHETFISH *ARGYROPELECUS* (STERNOPTYCHIDAE) IN THE EOCENE OF IRAN: DESCRIPTION AND PHYLOGENETIC RELATIONSHIPS OF TWO NEW SPECIES FROM THE PABDEH FORMATION

LORENZO RIDOLFI[1*], ALI BAHRAMI[2], MEHDI YAZDI[2], ANE ELISE SCHRØDER[1,3], GIUSEPPE MARRAMÀ[1] & GIORGIO CARNEVALE[1]

[1]Dipartimento di Scienze della Terra, Università degli Studi di Torino, Via Valperga Caluso, 35 I-1025 Torino, Italy.
[2]Department of Geology, Faculty of Sciences, University of Isfahan, POB. 81746-73441, Isfahan, I.R. Iran.
[3]Department of Geosciences and Natural Resource Management, University of Copenhagen, Øster Voldgade 10, 1350 Copenhagen K, Denmark.
*Corresponding author: lorenzo.ridolfi@unito.it

To cite this article: Ridolfi L., Bahrami A., Yazdi M., Schrøder A.E., Marramà G. & Carnevale G. (2025) - The deep-sea hatchetfish *Argyropelecus* (Sternoptychidae) in the Eocene of Iran: description and phylogenetic relationships of two new species from the Pabdeh Formation. *Rivista Italiana di Paleontologia e Stratigrafia*, vol. 131(3): 603-629.

Keywords: Teleostei; Stomiiformes; *Argyropelecus iranicus* n. sp.; *Argyropelecus zagrosensis* n. sp.; Bartonian; Zagros Basin.

Abstract: Two new deep-sea hatchetfish species, †*Argyropelecus iranicus* n. sp. and †*Argyropelecus zagrosensis* n. sp., are described in detail herein based on fossil material from the Eocene (Bartonian) deposits of the Pabdeh Formation, Zagros Basin, Iran. A detailed investigation of the skeletal morphology of these new species was made possible through elemental distribution maps obtained using µ-XRF imaging technique of the fossil material. These new species are the oldest known representatives of the genus *Argyropelecus*. A phylogenetic analysis that includes all the extant species of the genus *Argyropelecus* suggests that †*Argyropelecus iranicus* n. sp. and †*Argyropelecus zagrosensis* n. sp. pertain to the '*A. lychnus* species complex' and the '*A. affinis* species complex', respectively. The morphospace analysis confirmed the presence of two distinct morphotypes within the genus *Argyropelecus*. Potential correlations between morphospace occupation and the ecological setting and lifestyle of this bizarre group of deep-sea fishes are also discussed. The presence of two species of the genus *Argyropelecus* in the Eocene Pabdeh Formation extends the temporal and biogeographical range of these deep-sea fishes, providing additional information for our understanding of the evolutionary and biogeographical history of the deep-sea hatchetfishes.

http://zoobank.org/urn:lsid:zoobank.org:pub:2EBA9083-9061-4CBF-B19A-BD660914F6A6

Introduction

The Sternoptychidae is a well-recognized lineage of primarily mesopelagic fishes distributed worldwide and belonging to the order Stomiiformes (e.g., Kinzer & Schulz 1988). This family comprises ten extant (*Araiophos, Argyripnus, Argyropelecus, Danaphos, Maurolicus, Polyipnus, Sonoda, Sternoptyx, Thorophos, Valenciennellus*) and seven extinct genera (†*Archaeolicus,* †*Discosternon,* †*Eknomodophos,* †*Eosternoptyx,* †*Jerzmanskaephos,* †*Horbatshia,* †*Polyipnoides*) whose fossil record extends back to the Paleocene–Eocene boundary (e.g., Prokofiev 2002, 2005, 2010; Carnevale 2008; Afsari et al. 2014; El-Sayed et al. 2021). Among sternoptychids, the deep-sea hatchetfishes represent a well-defined clade, the Sternoptychinae, characterized by a peculiar set of morphological features, including a deep and extremely compressed body, mouth nearly vertical, eyes telescopic, abdominal keel-like structure, dorsal blade-like structure in front of the dorsal fin, and a vertically oriented pelvic girdle (e.g., Schultz 1938, 1961, 1964;

Received: June 16, 2025; accepted: September 03, 2025

Fig. 1 - Location of the fossil site of Babaheydar in the Zagros basin, near Isfahan, Iran, marked by a red star. Scale bar equals 10 km.

Baird 1971; Baird & Eckardt 1972; Weitzman 1974; Ahlstrom et al. 1984; Harold 1993, 1994; Harold & Weitzman 1996; Carnevale 2003, 2008).

The genus *Argyropelecus* includes seven extant species showing a broad range of body morphologies, from slender to deep bodies, all exhibiting (type alpha) photophores, which play a key role in counter-illumination (Baird 1971; Baird & Eckardt 1972; Weitzman 1974; Mensinger & Case 1990; Hoar et al. 1997; Priede 2017). *Argyropelecus* species commonly occur at depths from 100 to 600 meters and are known for their vertical migrations, primarily to feed on amphipods, copepods, euphausiids, and ostracods (e.g., Schultz 1938, 1961, 1964; Baird 1971; Hopkins & Baird 1973, 1985; Kinzer & Schulz 1988).

The fossil record of *Argyropelecus* dates back to the Oligocene, with the species †*Argyropelecus priscus* from the Czech, Polish and Romanian Carpathians and Caucasus (e.g., Cosmovici & Pauca 1943; Danil'chenko 1960, 1962; Jerzmańska 1968; Ciobanu 1977; Gregorová 1993; Prokofiev 2002, 2005). The Miocene record comprises the Paleomediterranean species †*Argyropelecus logearti* from the Algeria and Italy (Arambourg 1929; Carnevale 2003, 2007; Gaudant et al. 2015), and the Eastern Pacific species †*A. bullockii* and †*A. affinis* from the Modelo and Monterey formations in California (e.g., David 1943; Baird 1971). The extant species *A. hemigymnus* is known from abundant material from Pliocene and Pleistocene deposits of the Mediterranean basin (e.g., Landini & Menesini 1978, 1986; Sorbini 1988; Landini & Sorbini 1993).

The goal of this study is to describe two new species of *Argyropelecus* from the Eocene Pabdeh Formation, Zagros Basin, Iran, and to discuss their phylogenetic relationships.

Geological setting

The Babaheydar fossil locality is located not far from the city of Shahr-e Kord, less than 100 km southwest of Isfahan, central Iran. At this locality, the carbonates of the Pabdeh Formation are well exposed, including a number of productive fossiliferous layers (Fig. 1) that are renowned for their well-preserved fossils, including fishes, crustaceans, insects and plants (e.g., Garassino et al. 2014).

The first fossil fishes from the Pabdeh Formation were discovered by Roland de Mecquenem in 1904 and described by Priem (1908). Thirty years later, Camille Arambourg conducted extensive excavations on two sites where the Pabdeh Formation is well-exposed and discovered abundant material among which more than 30 fish taxa were recognized (Arambourg 1967). Subsequently, several studies have been focused on the fossil fishes from the Pabdeh Formation, including those by Haghipour & Brants (1971), Bannikov & Tyler (1995), Jafarian et al. (2000), Tyler (2000), Tyler et al. (2006), Bannikov et al. (2010), Afsari et al. (2014), Přikryl & Bannikov (2014), Přikryl et al. (2016), Davesne (2017), Bannikov (2018), and Carnevale & Tyler (2018).

The Pabdeh Formation is composed of thin- to thick-bedded marly limestones alternating with dark to light gray shales, rich in planktonic microfauna (Mohseni & Al-Asam, 2004; Mohseni et al. 2011), which accumulated in the northwestern and southern parts of the Zagros Basin between the late Paleocene and the Oligocene (James & Wynd 1965; Sampò, 1969). Overall, the sediments of the Pabdeh Formation mostly accumulated under oxygen-depleted conditions in the deeper portions of intrashelf basins (e.g., Ala et al. 1980; Murris 1980; Mohseni et al. 2011).

The fossiliferous layers of the Pabdeh Formation were erroneously referred by Arambourg (1967) to the Rupelian, based on the presence of certain fish taxa such as †*Bregmaceros filamentosus* Priem, 1908 and †*Palaeorhynchus*, which at that time were only known from the Oligocene of the Rhine Basin, Switzerland, the Carpathians, and Northern Caucasus. These taxa, however, were later found in several Eocene deposits of Europe (e.g., Bannikov 2010). According to Garassino et al. (2014), the planktonic foraminiferan assemblages of the fossiliferous horizons include †*Hantkenina alabamaensis* Cushman, 1925, †*H. compressa* Parr, 1947 and †*Morozovelloides bandyi* (Fleisher 1974). According to Coxhall & Pearson (2006), the range of these *Hantkenina* species spans from the Bartonian to the Eocene–Oligocene boundary, from about 41 to 33.9 Ma. †*Morozovelloides bandyi* is known to occur up to about 40 Ma (Payros et al. 2015), thereby suggesting that the fossiliferous horizons date back to the lower part of the Bartonian.

Materials and methods

Studied specimens

The present study is based on museum collection material from the mid-Eocene (Bartonian) Pabdeh Formation, Zagros Basin, Iran. It is deposited in the collections of the Department of Geology, Faculty of Sciences, University of Isfahan. The studied material comprises five nearly complete, well-preserved specimens IUGM 100892, IUGM 100893 (holotype designated herein), IUGM 100894, IUGM 100895, IUGM 100896 (holotype designated herein).

The fossils were examined using a Leica M80 stereomicroscope equipped with a camera lucida drawing arm. Measurements were taken to the nearest 0.1 mm using a dial caliper. Standard length (SL) is used throughout. Anatomical terminology and comparative data are mostly based on Baird (1971, 1986), David (1943), Weitzman (1974), Harold (1993, 1994, 1998), Carnevale (2003, 2007, 2008), Prokofiev (2002, 2005), and Afsari et al. (2014). Photophore terminology follows Harold (1994).

Analyses

We performed μXRF-analyses using a Bruker M4 Tornado Plus Amics benchtop device with a maximum acceleration voltage of 50 kV and an anode current of 600 μA (see Schrøder et al. 2023; Schrøder & Carnevale 2023). Pixel size was set to 25 μm and spot size to 20 μm. The dwell time was adjusted to the size of each specimen, including the area of interest, and varied between 8 to 16 ms/pixel. Hence, the overall acquisition times for the fossil specimens ranged from 3.03 to 16.01 hours. We mapped calcium-, manganese-, phosphorus-, sulphur-, strontium-, and titanium-distributions in the surface of the specimens to expose morphological details. Strontium, calcium and phosphorous are associated with the skeletal anatomy of fossilized fishes (Schrøder et al. 2022, 2023; Schrøder & Carnevale 2023, 2025). Titanium is commonly related to preserved fossil melanosomes (see Schrøder et al. 2023, figures 12 and 13). Occasionally, manganese and sulphur may also reveal anatomical details, relating to various body morphology, apparently including photophores (sulphur). Kα distribution element maps were generated with the proprietary software of the Bruker M4 device. The digital 2D-element maps were directly applied for taxonomic analyses and descriptions.

To infer the taxonomic position of the new taxa within the sternoptychine lineage, we performed a phylogenetic analysis in which *Polyipnus*, *Sternoptyx* and nine species of *Argyropelecus* (including those described herein) represent our ingroup, whereas three non-sternoptychine sternoptychids (*Valenciennellus, Thorophos* and *Argyripnus*) represent the outgroups. The character (ch.) matrix consists of 64 morphological characters, 1–37 taken from Harold (1993) and 37–64 from Weitzman (1974) (see Appendix, Table S1). The matrix was compiled in MESQUITE v.3.03 (Maddison & Maddison 2008) and the phylogenetic analysis was performed in TNT 1.6 (Goloboff & Morales 2023) using traditional search with 1000 replicates, 100 random seeds, tree bisection and reconnection with

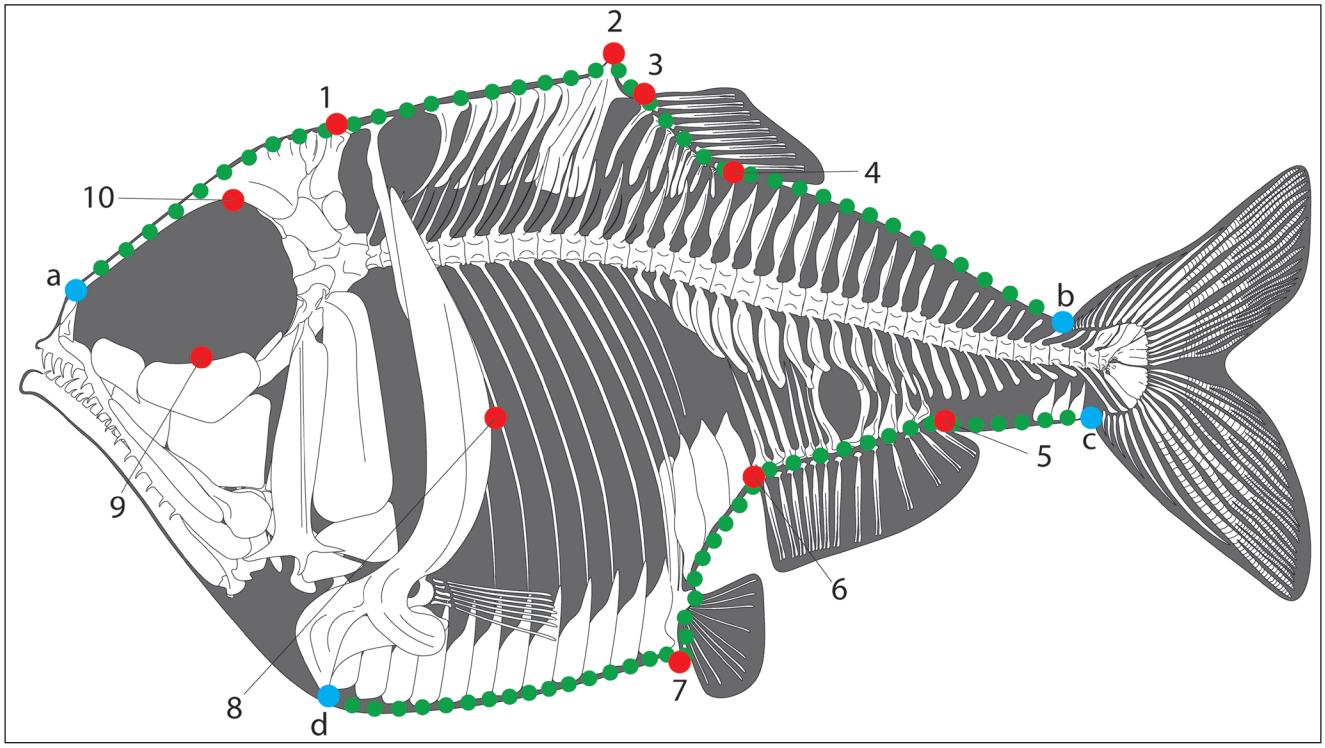

Fig. 2 - Landmarks and semilandmarks configuration. Landmarks represented by red dots are: 1) Dorsal tip of the supraoccipital; 2) tip of the dorsal blade; 3) anterior insertion of dorsal fin; 4) posterior end of dorsal fin; 5) posterior end of the anal fin; 6) anterior insertion of the anal fin; 7) ventralmost tip of the pelvic girdle; 8) point at the maximum of posterior curvature of the cleithrum; 9) ventralmost margin of the orbit; 10) dorsalmost point of the orbit (10). The anchor point landmarks, represented by light-blue dots, are: a) anterior tip of the frontals; b) insertion of the anteriormost dorsal procurrent ray; c) insertion of the anteriormost ventral procurrent ray; d) ventral tip of the cleithrum (d). Semi-landmarks are represented by 80 green dots.

ten trees saved per replication and collapsing trees after search. All characters were unordered and giving equal weight. Tree length, consistency (CI), and retention (RI) indices were calculated.

In order to quantify the morphological variability between the *Argyropelecus* species within the Sternoptychidae, we analysed the morphospace occupation of the two *Argyropelecus* complexes and compared it with that of selected genera of the family through geometric morphometrics (Zelditch et al. 2004). In this perspective, images of the extant taxa were obtained from the online picture repository of FishBase (http://www.fishbase.org; Froese & Pauly 2015) whereas images of the fossil taxa were taken from the literature. Our dataset includes a sample of 97 specimens, representing nine genera and 28 species. A total of 14 landmarks (of which four are anchor points for intervening semilandmarks) and 80 equidistant semilandmarks describing the dorsal and ventral profile of body (Fig. 2) were digitized using the software TPSdig 2.32 (Rohlf 2005). Landmarks were selected based on their potential ecological or functional role in the Sternoptychidae, as suggested by previous studies on representatives of this family (Baird 1971; Weitzman 1974; Harold 1993; Gordeeva & Nanova 2017; May 2019). The coordinates of the landmarks were subjected to translation, rotation, and scaling to a unit centroid size by performing a Generalized Procrustes Analysis (GPA). This procedure was employed to minimize any variation induced by factors such as size, orientation, location, and rotation (Rohlf & Slice 1990; Zelditch et al. 2004). The Generalized Procrustes Analysis (GPA) was performed using the TPSrelw software package (Rohlf 2003), followed by a principal component analysis (PCA) of the Procrustes coordinates to obtain the Relative Warp (RW). Shape variations were visualized along the axes using deformation grid plots. The non-parametric multivariate analysis of variance (PERMANOVA; Anderson 2001) and the analysis of similarities (ANOSIM; Clarke 1993) were performed using the software packages PAST 5.2 (Øyvind & Harper 2001) to assess significant differences in morphospace occupation between groups. Euclidean distance was used as the metric for both tests, and statistical significance along the first three RW axes was assessed using 9,999 random permutations.

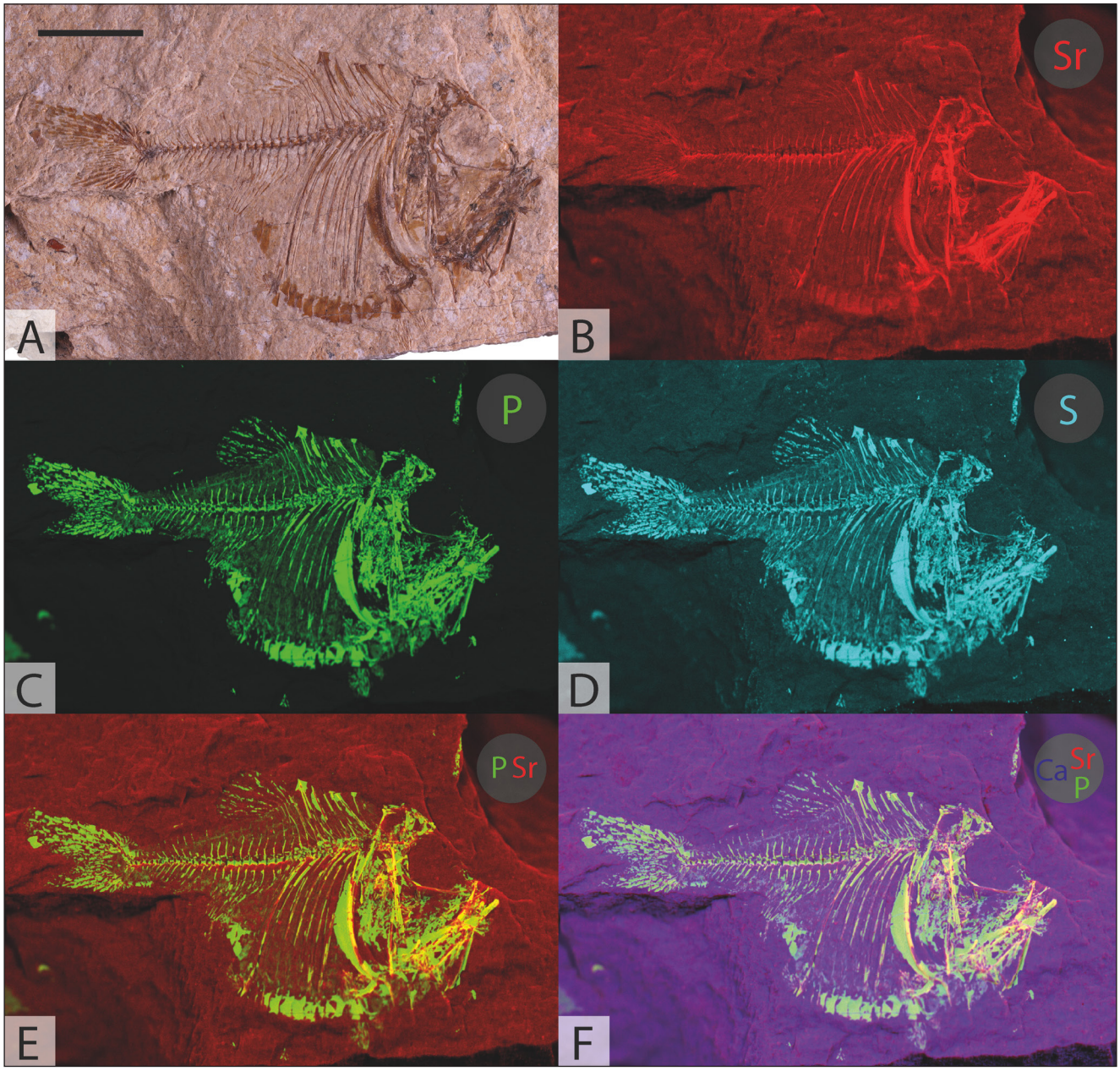

Fig. 3 - †*Argyropelecus iranicus* n. sp., holotypic part, IUGM 100896, from the Eocene of Babaheydar. A) high-resolution photo image; B) strontium element map; C) phosphorous element map; D) sulfur element map; E) combined element map of strontium and phosphorous; F) combined element map of strontium (red), phosphorous (green) and calcium (blue). Scale bar equals 10 mm.

To assess whether correlation occurs between shape and vertical distribution in the water column, we performed a Partial Least Squares (PLS) analysis using the software TPSpls (Rohlf & Corti 2000). Data on the vertical distribution of the living species was obtained from the databases iNaturalist (https://www.inaturalist.org/) and FishBase (http://www.fishbase.org; Froese & Pauly 2015) and literature (Baird 1971). To investigate which of the RW axes or couple of variables concur with most of the correlation, we performed a collinearity analysis on the first three RWs using the GEMMA toolbox for R (version 4.5.0) (Pilade et al. 2025). Alpha (level of significance) was set to 0.05 for all tests.

Systematic palaeontology

Order **Stomiiformes** *sensu* Harold & Weitzman, 1996
Infraorder **Gonostomata** *sensu* Harold, 1998
Family Sternoptychidae Duméril, 1805

Genus *Argyropelecus* Cocco, 1829

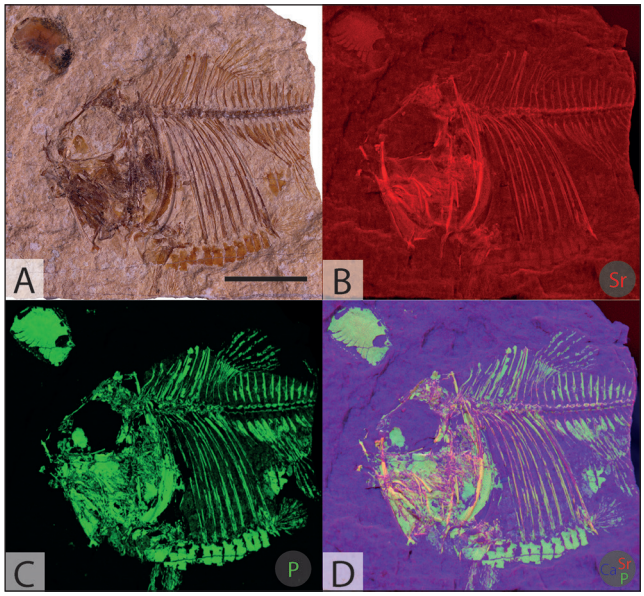

Fig. 4 - †*Argyropelecus iranicus* n. sp., holotypic counterpart, IUGM 100896 from the Eocene of Babaheydar. A) high-resolution photo image; B) strontium element map; C) phosphorous element map; D) combined element map of strontium (red), phosphorous (green) and calcium (blue). Scale bar equals 10 mm.

†*Argyropelecus iranicus* n. sp.

Figs. 3-14

Derivation of the name: From Iran, the country where the described specimens were discovered.

Diagnosis: A deep-bodied species of *Argyropelecus* unique in having the following combination of features: head length ranging from 39.2% to 41.6% of SL; body depth between 68.2% and 71.8% of SL; frontals slightly ornamented in the posterior region, other head bones only feebly ornamented; parietals do not contact the sphenotic ventrally; preopercle bearing two spines almost perpendicular to each other; vertebral column containing 36 vertebrae (15 precaudal and 21 caudal); anterior caudal vertebrae bearing expanded and spatulate neural and haemal spines; ten pairs of ribs, the two posterior notably shorter; dorsal blade oriented subvertically and moderately protruding from the dorsal margin of the body; dorsal fin includes nine rays supported by eight pterygiophores; anal fin with 13 rays supported by 12 pterygiophores; basipterygium elongated, bearing a slightly curved ischial process and a broad and ventrally directed iliac process; single iliac spine thick and vertically oriented; anal hiatus broad and almost ovoid in outline; hypurals 1 and 2 completely coalescent; three VAV photophore scales present, located behind the robust abdominal keel along the ventral margin of the body.

Holotype: IUGM 100896, a nearly complete articulated skeleton, in part and counterpart, 37.6 mm SL. The counterpart is incompletely preserved, missing the caudal region (Fig. 3–4).

Paratypes: IUGM 100895, a nearly complete articulated skeleton, 36.0 mm SL (Fig. 5); IUGM 100894, a nearly complete articulated skeleton, 36.8 mm SL (Fig. 6).

Horizon and Locality: Pabdeh Formation, Upper Eocene; Babaheydar, Zagros Basin, Iran.

Measurements (as % SL)*:* Total length: 123.2–130.0; head length: 39.2–41.6; head depth: 58.1–65.7; snout length: 1.8–2.2; orbit diameter: 13.5–14.4; maximum body depth: 68.2–71.8; caudal peduncle length: 12.2–12.7; caudal peduncle depth: 11.2–12.8; predorsal length: 52–56.3; preanal length: 70.1–71.5; prepectoral length: 32.1–35.5; prepelvic length: 63.5–64.5; dorsal-fin base length: 8.6–9.7; anal-fin base length: 10.1–13.8. (Table 1)

Description

The body is deep and laterally compressed (Fig. 7), its maximum depth is located just in front of the dorsal-fin origin, tapering steeply posterior to the pelvic fins. Overall, the skeleton is well-ossified. The length of the postpelvic region of the body equals that of the prepelvic region. The head is remarkably deep, reaching its maximum depth at the level of the supraoccipital crest. The orbit is large and oblong. The highly modified supraneurals produce a blade-like predorsal profile. The anal fin is short and originates just behind the dorsal-fin base. Overall, this combination of body traits resembles that of the extant species *Argyropelecus olfersii, A. sladeni,* and *A. lychnus.*

The head (Fig. 8) is contained about 2.5 times in SL. The neurocranium is deep and robust. The ethmoid region is inadequately preserved, due to its prevalent cartilaginous nature (see Weitzman 1974; Carnevale 2003, 2008) but IUGM 100894 exhibits both the supraethmoid and lateral ethmoid, the only two ossified elements of this region in the genus *Argyropelecus*. The supraethmoid articulates posterodorsally with the frontals, and posteroventrally with the lateral ethmoid. The lateral ethmoid is short, well-ossified and slightly concave posteriorly, forming the anterior border of the orbit. The robust and well-developed frontals are the largest bones of the skull roof. They articulate with the supraethmoid anteriorly and form the dorsal margin of the orbit, becoming expanded posteriorly, where they articulate with the bones of the otic region and the parietals. The longitudinal frontal fossa is flat and separated anteriorly, resembling the condition typical of the species of the '*A. lychnus* complex' of Baird (1971). The outer surface of the frontals lacks pits, although some shallow ridges can be observed in the posterior region along the frontal crest. The absence of pits might be considered as a primitive trait since several extant species display a more pronounced ornamentation (Baird 1971; Weitzman 1974). The parietals are almost triangular in outline and bear a median ridge (see Baird 1971; Weitzman 1974; Harold 1993), which is continuous with the frontal crest. The supraoccipital is well developed and articulates with the parietals anteriorly and with the

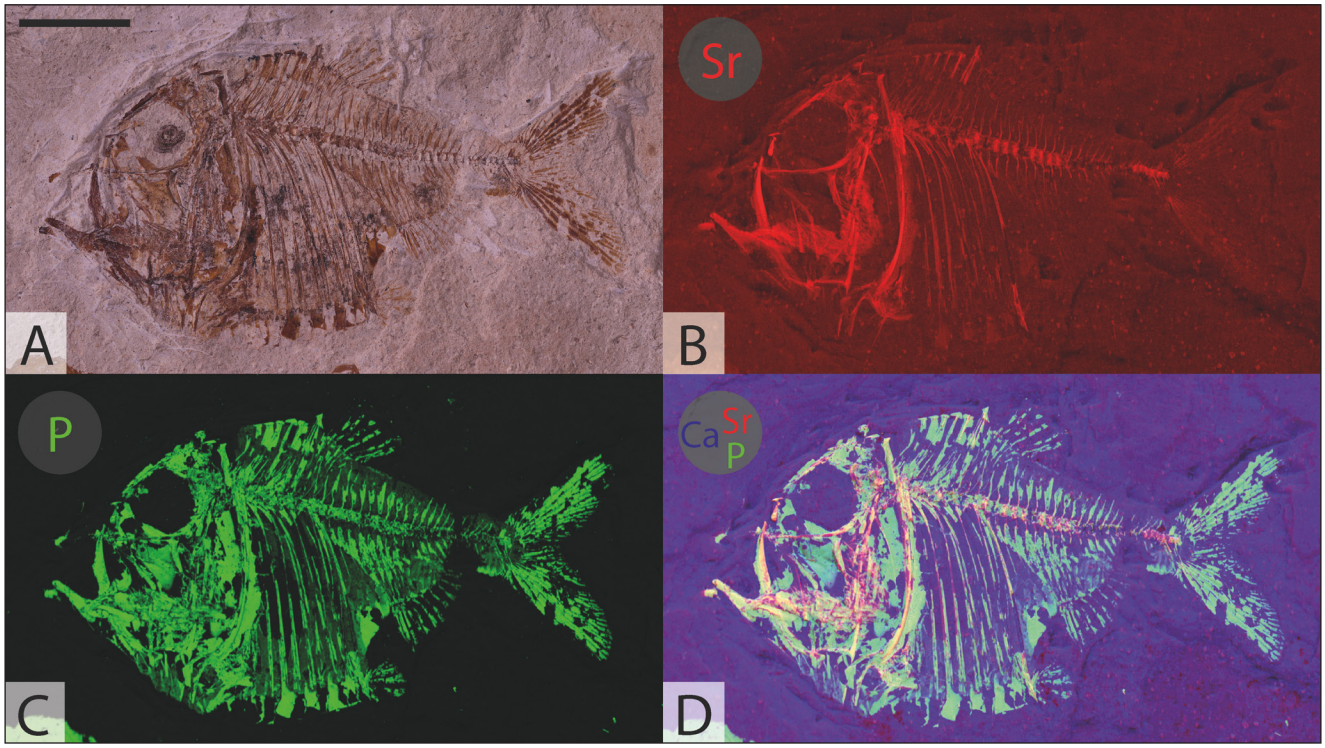

Fig. 5 . †*Argyropelecus iranicus* n. sp., paratype, IUGM 100895, from the Eocene of Babaheydar. A) high-resolution photo image; B) strontium element map; C) phosphorous element map; D) combined element map of strontium (red), phosphorous (green) and calcium (blue). Scale bar equals 10 mm.

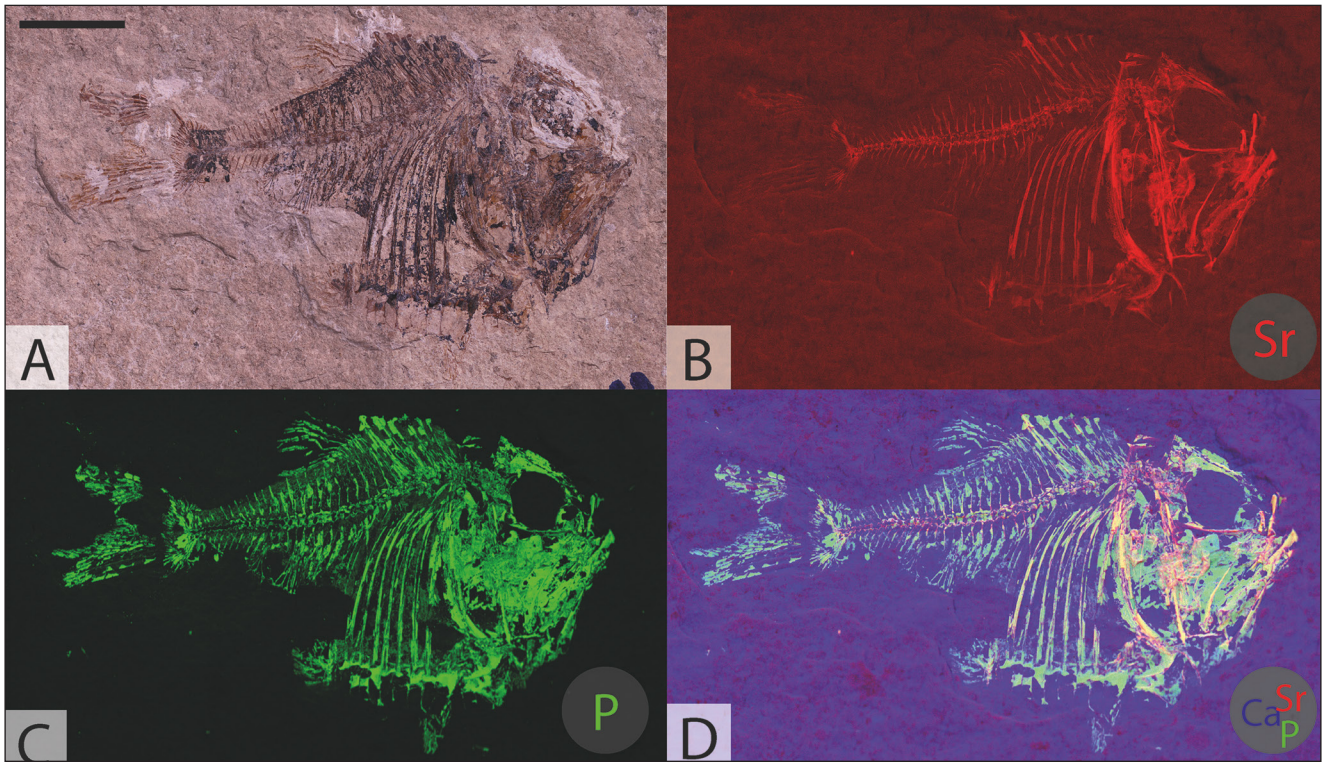

Fig. 6 - †*Argyropelecus iranicus* n. sp., paratype, IUGM 100894, from the Eocene of Babaheydar. A) high-resolution photo image; B) strontium element map; C) phosphorous element map; D) combined element map of strontium (red) phosphorous (green) and calcium (blue). Scale bar equals 10 mm.

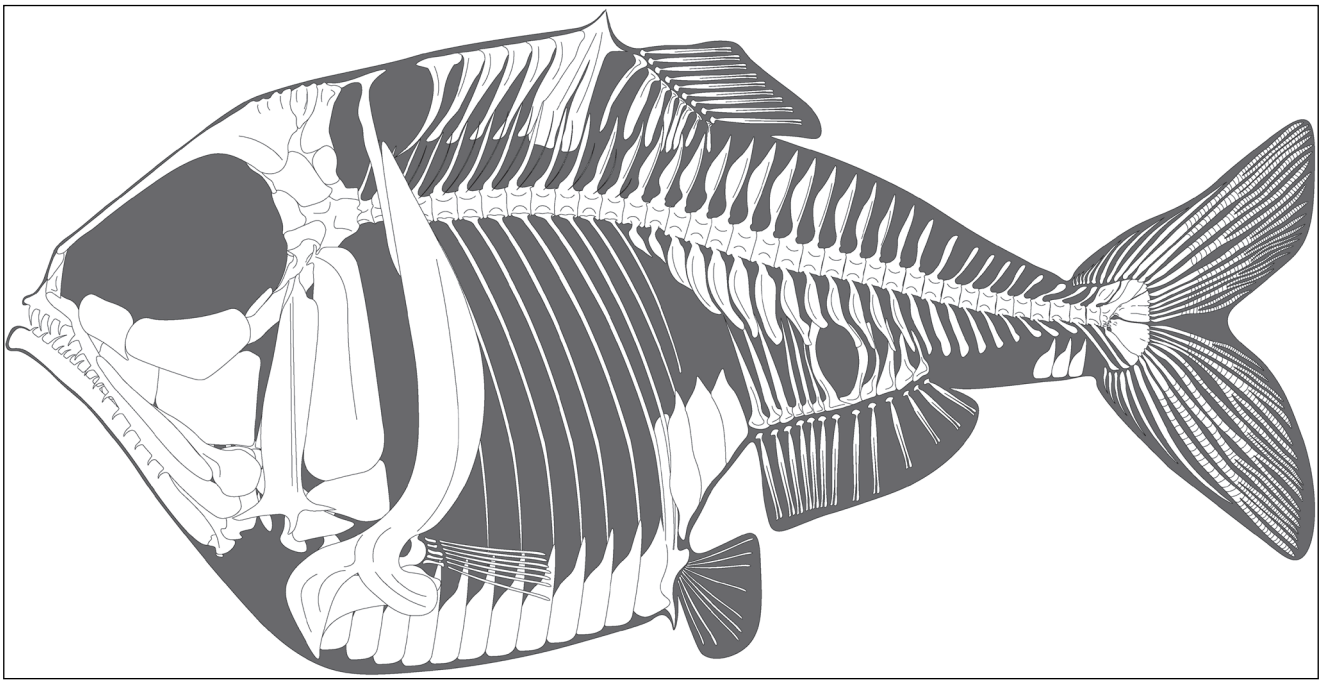

Fig. 7 - Interpretative reconstruction of the whole skeleton of †*Argyropelecus iranicus* n. sp. from the Eocene of Babaheydar, based on IUGM 100894, IUGM 100895, and IUGM 100896.

fused posttemporal and supracleithrum posteriorly. The outline of the pterotic is difficult to recognize as the otic area is poorly preserved. The sphenotic is moderately ornamented with an irregular shape; this bone does not reach the ventral margin of the parietal and articulates with the pterosphenoid medially, and the prootic ventrally. The exoccipital and epioccipital are poorly preserved. The basioccipital is small, similar in shape to that of *Argyropelecus affinis* (see Weitzman 1974). The parasphenoid is long and strongly arched and bears a ventral keel as the other species of the genus *Argyropelecus*; the anterior tip of the parasphenoid articulates with the vomer.

The orbit is large, oblong and occupies more than half of the head length and about one-third of its depth. The bones of the infraorbital series are incompletely preserved. The lachrymal is broad and subrectangular, whereas the second infraorbital is very large and occupies the central portion of the ventral border of the orbit. What appears to be another infraorbital is tubular in shape, though its exact identity remains unclear due to its taphonomic displacement. The other infraorbitals are difficult to recognize.

The mouth is strongly oblique. Numerous well-spaced conical teeth with recurved tips are present along the alveolar surface of the premaxilla, maxilla and dentary. The premaxilla is small and subtriangular and bears a well-developed ascending process, similar to that of other *Argyropelecus* species. The maxilla is robust, elongate and gently curved; it occupies 70% of the total length of the head. There are two supramaxillae. The first one is elongate and slender, bordering most of the dorsal margin of the maxilla. The posterior supramaxilla is drop-shaped and located along the posterior edge of the maxilla. The lower jaw is elongated and triangular in shape, not protruding significantly beyond the maxilla. The ventral margin of the dentary is gently concave. The anguloarticular is almost triangular in shape. The small retroarticular is partially hidden by the anguloarticular. The outline of the lower jaw shows remarkable similarities to that of *A. lychnus* described in detail by Baird (1971).

The suspensorium consists of the hyomandibula, quadrate, symplectic, metapterygoid, endopterygoid, ectopterygoid, and palatine. The hyomandibula consists of a rod-shaped vertical shaft bearing an anterior spine (see Weitzman 1974; Carnevale 2003), and a thick dorsal articular head. The quadrate is deeper than wide, articulating with the anguloarticular through its robust articular condyle. The symplectic is difficult to recognize in the available specimens. The metapterygoid is the largest bone

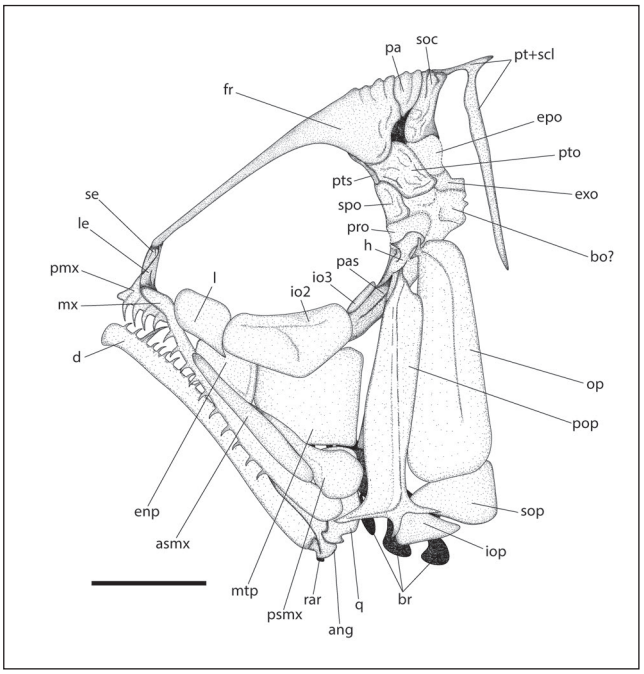

Fig. 8 - Interpretative reconstruction of the head of †*Argyropelecus iranicus* n. sp. from the Eocene of Babaheydar, based on IUGM 100894, IUGM 100895, and IUGM 100896. Abbreviations: ang: angular, asmx: anterior supramaxilla, bo: basioccipital, br: branchiostegal ray, d: dentary, enp: endopterygoid, epo: epioccipital, exo: exoccipital, l: lachrymal, fr: frontal, h: hyomandibular, io: infraorbital bones, iop: interopercle, le: lateral ethmoid, mtp: metaptererygoid, mx: maxilla, op: opercle, pa: parietal, pas: parasphenoid, pmx: premaxilla, pop: preopercle, pt+scl: posttemporal+supracleithrum, pro: prootic , psmx: posterior supramaxilla, pto: pterotic, pts: pterosphenoid, q: quadrate, rar: retroarticular, se: supraethmoid, soc: supraoccipital, spo: sphenotic, sop: subopercle. Scale bar equals 10 mm.

of the suspensorium; it is trapezoidal in shape with a more ossified posterodorsal region. It contacts the endopterygoid anteriorly, the ectopterygoid anteroventrally, and the quadrate ventrally. The endopterygoid is smaller and almost rectangular in outline. The boomerang-shaped ectopterygoid is visible only in IUGM 100895. The palatine is only partially exposed in the available material; it is not possible to determine whether one or more rows of palatine denticles are present as in extant *Argyropelecus* species (Baird 1971; Weitzman 1974).

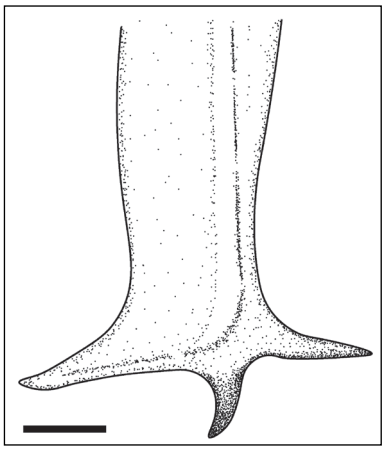

Fig. 9 - Interpretative reconstruction of the distal portion of the preopercular bone of †*Argyropelecus iranicus* n. sp. from the Eocene of Babaheydar, based on IUGM 100894, IUGM 100895, and IUGM 100896. Scale bar equals 2 mm.

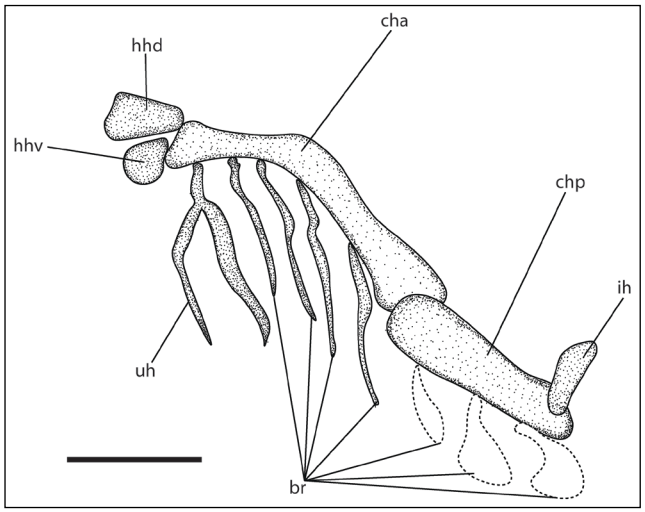

Fig. 10 - Interpretative reconstruction of the hyoid apparatus of †*Argyropelecus iranicus* n. sp. from the Eocene of Babaheydar based on IUGM 100894, IUGM 100895, and IUGM 100896. Abbreviations: br: branchiostegal ray, cha: anterior ceratohyal, chp: posterior ceratohyal, hhd: dorsal hypohyal, hhv: ventral hypohyal, ih: interhyal, uh: urohyal. Scale bar equals 5 mm.

The opercular series consists of vertically elongated bones, resembling those of the other congenerics. The preopercle (Figs. 8–9) is deep and narrow, L-shaped, with a short anterior arm; the laterosensory canal is covered by a well-ossified lamella originating from the medial ridge. Like in †*Argyropelecus logearti* and *A. sladeni* (see Baird 1971), the preopercle bears two spines perpendicular to each other, one of which is robust, stout and vertically oriented, the other being slender and longer, extending posteriorly just beyond the posterior edge of the preopercle (Fig. 9). The opercle is vertically oriented, subrectangular in shape and covers approximately two-thirds of the head depth; it shows a thick median ridge but there is no evidence of pits on the surface. The subopercle is small and subtriangular in outline and lies ventral to the opercle. The interopercle is visible only in the holotype; it has a subtriangular outline and is located beneath the ventral end of the preopercle.

The hyoid apparatus (Fig. 10) is inadequately preserved. The dorsal hypohyal is slightly larger than the ventral hypohyal. The anterior ceratohyal is narrow, elongate, and expanded posteriorly; it has a concave ventral margin that supports at least four branchiostegal rays. The posterior ceratohy-

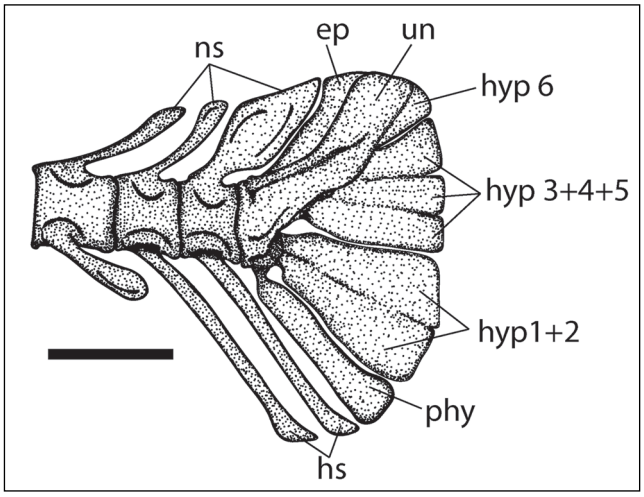

Fig. 11 - Interpretative reconstruction of the caudal skeleton of †*Argyropelecus iranicus* n. sp. from the Eocene of Babaheydar, based on IUGM 100894, IUGM 100895, and IUGM 100896. Abbreviations: ep: epural, hyp: hypural, hs: haemal spine, ns: neural spine, phy: parahypural, un: uroneural. Scale bar equals 5 mm.

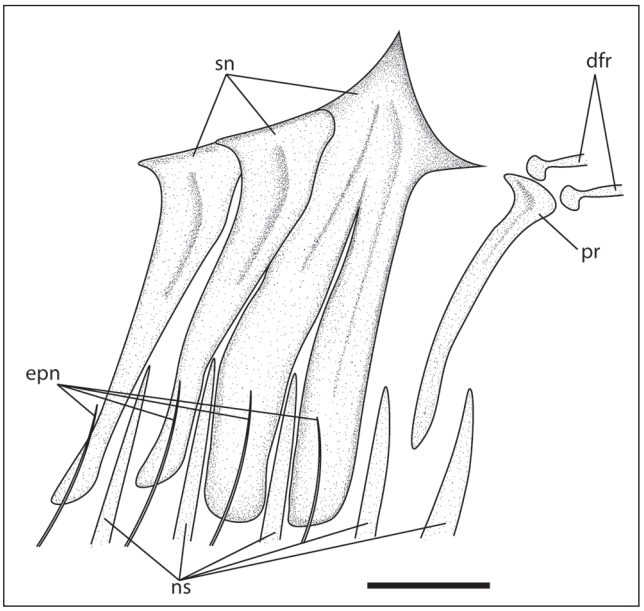

Fig. 12 - Interpretative reconstruction of the dorsal blade skeleton of †*Argyropelecus iranicus* n. sp. from the Eocene of Babaheydar based on IUGM 100894, IUGM 100895, and IUGM 100896. Abbreviations: dfr: dorsal fin ray, epn: epineural, ns: neural spine, pr: dorsal-fin pterygiophores, ep: epural, hyp: hypural, hs: hemal spine, ns: neural spine, phy: parahypural, sn: supraneural un: uroneural. Scale bar equals 5 mm.

al is smaller than the anterior ceratohyal; it slightly exceeds the half of the length of the anterior ceratohyal and bears at least three robust, expanded, plate-like branchiostegal rays. The urohyal is well-developed and ossified, nearly as long as the anterior ceratohyal; it is distally forked, resembling the Y-shape morphology described by Baird (1971), with the ventral portion being longer and lacking flanges or laminae.

The vertebral column consists of 36 vertebrae of which 15 are abdominal and 21 are caudal. The vertebral column is sub-horizontal, exhibiting only a slight kyphotic curve at the transition between the abdominal and caudal vertebrae, resembling the condition of deep-bodied *Argyropelecus* species*, A. olfersii* (Cuvier, 1829), *A. sladeni* (Regan, 1908) and *A. lychnus* (Garman, 1899) (see Baird 1971). The abdominal portion consists of robust vertebrae, the most anterior ones being higher than long and becoming subquadrangular in shape posteriorly in the series. The anterior caudal vertebrae are subquadrangular in shape, becoming progressively more elongate from the twelfth vertebra backward. The neural and haemal spines are prominent, those in the central portion of the vertebral column are remarkably expanded and spatulate. The neural spines of the vertebrae of the caudal peduncle are thinner and shorter. The haemal spines of the eighth, ninth and tenth caudal vertebrae are modified to accommodate the anal hiatus, which houses the large anal photophore (as in the '*Argyropelecus lychnus* complex' species; Baird 1971). The four posterior abdominal vertebrae bear expanded parapophyses gradually increasing in size posteriorly. Ten pairs of ribs occur on the abdominal vertebrae from the third backward; the eight anterior ribs are enlarged and extend ventrally to reach the specialized scales along the ventral margin of the body, or, the pelvic girdle, whereas the two posterior ribs are thinner and shorter and placed behind the pelvic girdle. Eight epineurals can be observed in the holotype, while IUGM 100895 has 11.

The caudal skeleton (Fig. 11) is robust and well-ossified. The first preural centrum and two ural centra are fused into a single compound centrum. The parhypural is autogenous without a parhypurapophysis. The hypurals are autogenous. The first and the second hypurals are fused at least proximally. Co-ossification of the first and second hypurals has been observed in several *Agyropelecus* species (e.g., *Argyropelecus aculeatus, A. hemigymnus, A. lychnus, A. olfersii* and, *A. sladeni*; Weitzman 1974). However, it is unclear whether the third, fourth, and fifth hypurals are fused to each other or not; the sixth hypural is separate from the other upper hypurals. A thick uroneural is fused with the compound cen-

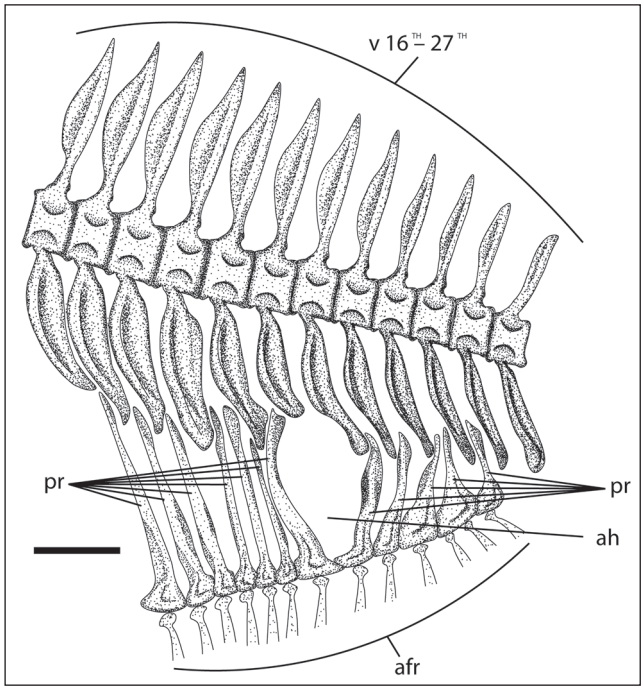

Fig. 13 - Interpretative reconstruction of the postabdominal region and anal fin region, showing the modified structure hosting the anal hiatus of †*Argyropelecus iranicus* n. sp. from the Eocene of Babaheydar based on IUGM 100894, IUGM 100895, and IUGM 100896. Abbreviations: afr: anal fin rays, ah: anal hiatus, pr: anal-fin pterygiophores, v: vertebrae. Scale bar equals 5 mm.

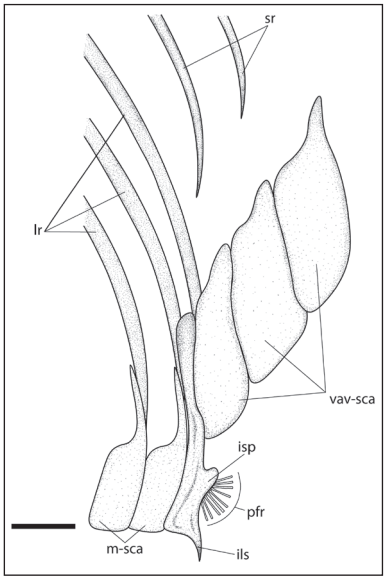

Fig. 14 - Interpretative reconstruction of the pelvic girdle of †*Argyropelecus iranicus* n. sp. from the Eocene of Babaheydar based on IUGM 100894, IUGM 100895, and IUGM 100896. Abbreviations: ils: iliac spine, isp: ischial process, lr: long ribs, m-sca: modifed scales, pfr: pelvic fin rays, sr: short ribs, vav-sca: VAV scales. Scale bar equals 5 mm.

trum. There is a single flat and anteroposteriorly expanded epural that is partially covered by the uroneural. The caudal fin is forked, with subequal lobes and there are 19 (9+10) principal, distally bifurcate, caudal-fin rays. There are at least ten dorsal and six ventral procurrent rays.

The dorsal fin (Fig. 12) is preceded by eight anteroposteriorly expanded supraneurals. The first supraneural is notably curved whereas the others are more straight and obliquely oriented. Each supraneural is expanded distally and together form a robust dorsal blade. The two posterior supraneurals are fused distally, forming the dorsal tip of the dorsal blade that protrudes from the dorsal margin of the body, following a subvertical direction (as in *Argyropelecus gigas, A. lychnus, A. olfersii, A. sladeni,*†*A. bulloki* and †*A. priscus*). The dorsal fin consists of nine distally bifurcated rays supported by eight robust pterygiophores, with the first one also supporting a supernumerary ray.

The anal fin is well-preserved only in IUGM 100895. It consists of 13 distally bifurcated rays supported by 12 pterygiophores. The first anal-fin ray is supernumerary on the first pterygiophore. Each pterygiophore has a thick central axis that bears anterior and posterior bony laminae (Fig. 13); the anteriormost six pterygiophores are long and straight, while the seventh and eighth are notably curved due to the presence of the anal hiatus in between, which is a synapomorphy shared by all the *Argyropelecus* species (Baird 1971; Harold, 1993; Carnevale 2003).

The pectoral girdle is deep and robust; the outer surface of its bones is extensively ornamented with numerous pits of different sizes and shapes. The posttemporal is fused with the supracleithrum (Fig. 8) as in other *Argyropelecus* species (Weitzman 1974; Carnevale 2003) and is in contact with the anterodorsal margin of the cleithrum. The cleithrum is the largest bone of the pectoral girdle; it is sigmoid in shape, with the dorsal portion being wider and much more developed than the ventral portion. The coracoid is hourglass-shaped. The scapula is pierced by a large scapular foramen. There are four pectoral-fin radials that articulate with at least seven rays (Table 1).

The pelvic fin consists of at least seven rays. The basipterygium (Fig. 14) is slender and vertically oriented, contacting the distal tips of the two posterior elongate ribs. The ischial process is more curved than that described by Weitzman (1974) for the extant *Argyropelecus* species. The iliac process and iliac spine are broad, well-ossified, and posteriorly directed. Only a single thick and ventrally oriented postabdominal spine can be recognized.

†*Argyropelecus iranicus* n. sp. lacks most of body scales as in other species of the genus *Argyropelecus* (Baird 1971; Harold 1993; Weitzman 1974; Carnevale 2003), the ventral margin of the body is charac-

	A. aculeatus	*A. affinis*	*A. gigas*	*A. hemigymnus*	*A. lychnus*	*A. olfersii*	*A. sladeni*	†*A. bullocki*	†*A. priscus*	†*A. logearti*	†*A. zagrosensis*	†*A. iranicus*
Measurements												
MaxSL	46	51	52	30	40	50	43	39	27	42	**31.6**	**37.6**
Body depth	38	23	29	17	28	34	25	61.5–78.5	60–74	85	**43.13–43.3**	**68.2–71.8**
Head length	14	15	17	10	14	16	14	46.2–50.5	40–43	33.3–41.5	**29.9–32.8**	**39.2–41.6**
Head depth	31	21	25	15	26	30	21	53.9–72.4	50–58	53.7	**35.5–37**	**58.1–65.7**
Predorsal distance	23	26	27	15	21	26	23	?	?	43.8–65.9	**48–50.7**	**52–56.4**
Preanal distance	30	31	32	17	25	32	28	?	?	68.8–80.5	**63.3–66.8**	**70.1–71.5**
Prepelvic distance	26	25	28	14	24	26	23	?	?	59.4–69	**48.7–48.8**	**63.5–64.5**
Counts												
Total vertebrae	34–36	38–40	38–39	36–39	36	36–38	35–37	37–38	35–36	38	**38**	**36**
Dorsal-fin rays	9	9	9–10	8	9	9	9	9	7–8	8	**8**	**9**
Anal fin rays	12	12–13	12–13	11	11–13	12	12	12	11–12	11	**10**	**13**
Pectoral-fin rays	9–11	11–12	11	9–11	10–11	10–11	10–11	11	?	9	**4+**	**7+**
Pelvic-fin rays	6	6	6	6	6	6	6	?	?	6	**5+**	**7+**
Iliac spines	2	2	2	1	2	2	2	2	2	1	**0**	**1**
VAV photophore scales	?	4+	?	4	4+	?	?	3+	?	4	**7**	**3**
Traits												
Parietal contact with sphenotic	No	Yes	Yes	No	No	No	No	?	?	No	Yes	No
Canine fan-like on lower jaw	Present	Present	Present	Absent	Present	Present	Absent	?	?	Absent	Absent	Present
Dorsal-fin blade	high	low	low	high	high	high	high	high	High	high	**low**	**high**
Ventral preopercular spine	Medium size	Long	Long	Medium size	Long	Long	Short	?	Short	Short	Long	Short
Posterior preopercular spines	Medium size	Short	Short	Medium size	Long	Short	Long	?	Medium size	Long	Short	Long
Anal hiatus region	Highly modified	Not very modified	Not very modified	Highly modified	Highly modified	Highly modified	Highly modified	Highly modified	Highly modified	Highly modified	Not very modified	Highly modified
Spines of postabdominal vertebrae	Spatulate	Slender	Slender	Spatulate	Spatulate	Spatulate	Spatulate	Spatulate	?	Spatulate	Slender	Spatulate

Tab. 1 - Summary of major morphological features of †*A. iranicus* n. sp., †*A. zagrosensis* n. sp. and other *Argyropelecus* species. Includes new data and data from Badcock (1984), Baird (1971,1986), Carnevale (2003), David (1943), Jerzmańska (1968), Schultz (1964).

terized by the presence of a robust abdominal keel made of 12 stiff bony scales, extending from the ventral margin of the coracoid to the anal-fin origin. Three of these modified scales are also visible just anterior to the caudal fin. These scales likely supported ventral bioluminescent photophores as in extant *Argyropelecus* species (Baird 1971; Baird & Eckardt 1972; Weitzman 1974; Mensinger & Case 1990; Hoar et al. 1997) (Figs. 3–6). What seems to be presence of possible soft tissue, especially in the abdominal region is evident in the P and S maps (Figs. 3–6). This is the area where extant *Argyropelecus* species exhibit a high number of photophores, which apparently also correlate with the elevated sulphur concentrations in the specimens (Fig. 3). In †*A. iranicus*, traces of the photophore indicate the presence of the abdominal series (AB), of the anal series (AN) in the anal hiatus region, as well as of the preanal (PAN), suprabdominal (SAB), and subcaudal series (SC) (see Baird 1971).

†*Argyropelecus zagrosensis* n. sp.

Figs. 15–23

Derivation of the name: The specific name refers to the Zagros Basin, Iran

Diagnosis: A narrow-bodied species of *Argyropelecus* that is unique by the following combination of features: head length ranging from 29.9% to 32.8% of SL; body depth between 43.1% and 43.3% of SL; frontals ornamented with short ridges in the posterior region, other head bones not ornamented; parietal articulating with the sphenotic ventrally; preopercle bearing two spines perpendicular to each other, the vertically-directed being longer; vertebral column comprising 38 vertebrae (15 abdominal and 23 caudal); neural and haemal spines of the anterior caudal vertebrae slender; nine pairs of ribs, the posterior of which is considerably shorter; tip of the dorsal blade only slightly protruding from the dorsal margin of the body; dorsal fin includes eight rays supported by seven pterygiophores; anal fin includes ten rays supported by nine pterygiophores; iliac spine absent; anal hiatus present, not involving strong modification of the anal-fin pterygiophores, similar to that of species of the '*Argyropelecus affinis* complex'; hypurals 1 and 2 fused at least proximally; seven specialized scales present along the ventral margin of the body between the pectoral girdle and the anal-fin origin.

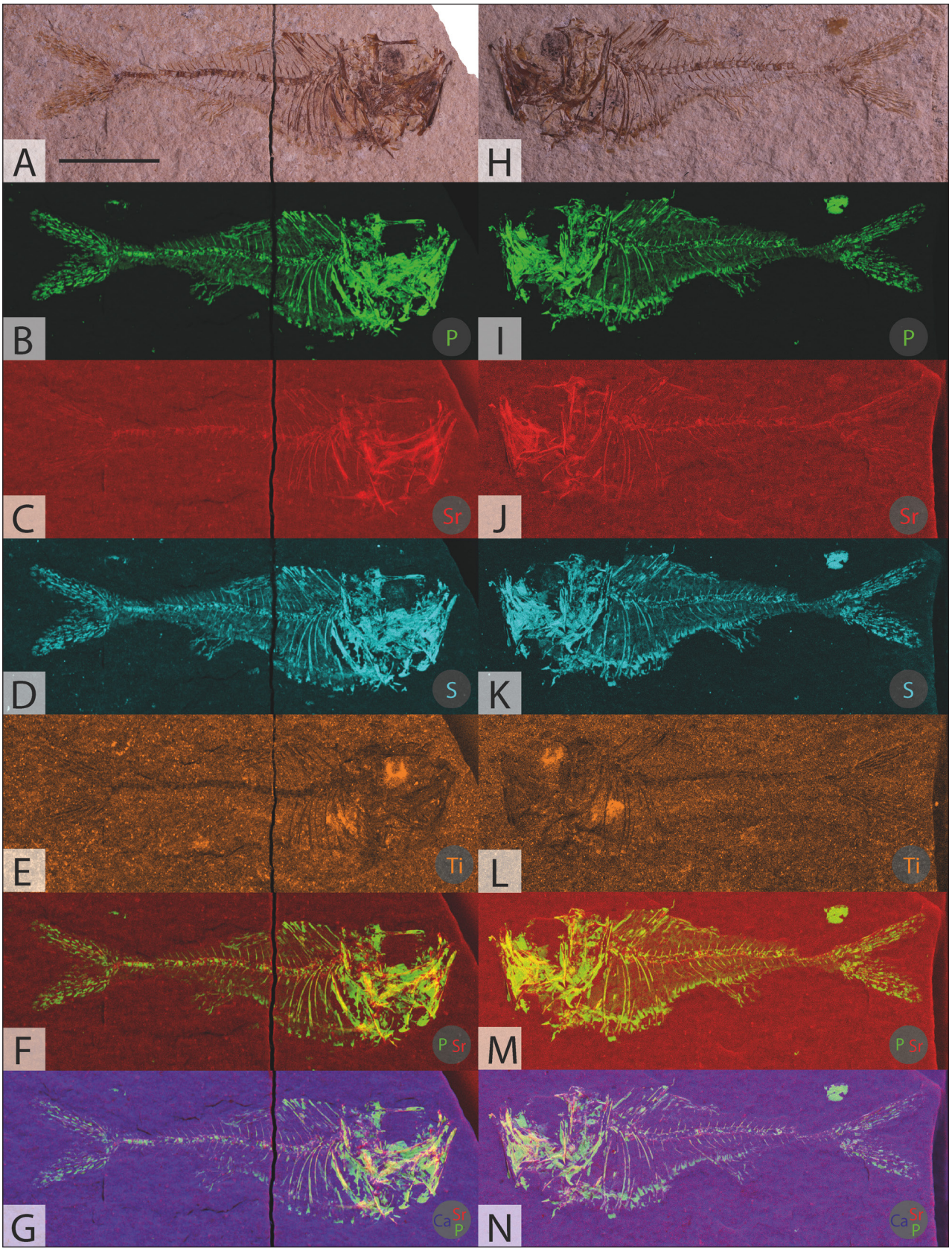

Fig. 15 - †*Argyropelecus zagrosensis* n. sp., holotype, IUGM 100893, in part and counterpart from the Eocene of Babaheydar. A) high-resolution photo image (part); B) phosphorous element map; C) strontium element map; D) sulfur element map; E) titanium element map; F) combined element map of strontium (red) and phosphorous (green); G) combined element map of strontium (red), phosphorous (green) and calcium (blue); H) high-resolution photo image (counterpart); I) phosphorous element map; J:) strontium element; K) sulfur element map; L) titanium element map; M) combined element map of strontium (red) and phosphorous (green); N) combined element map of strontium (red), phosphorous (green) and calcium (blue). Scale bar equals 10 mm.

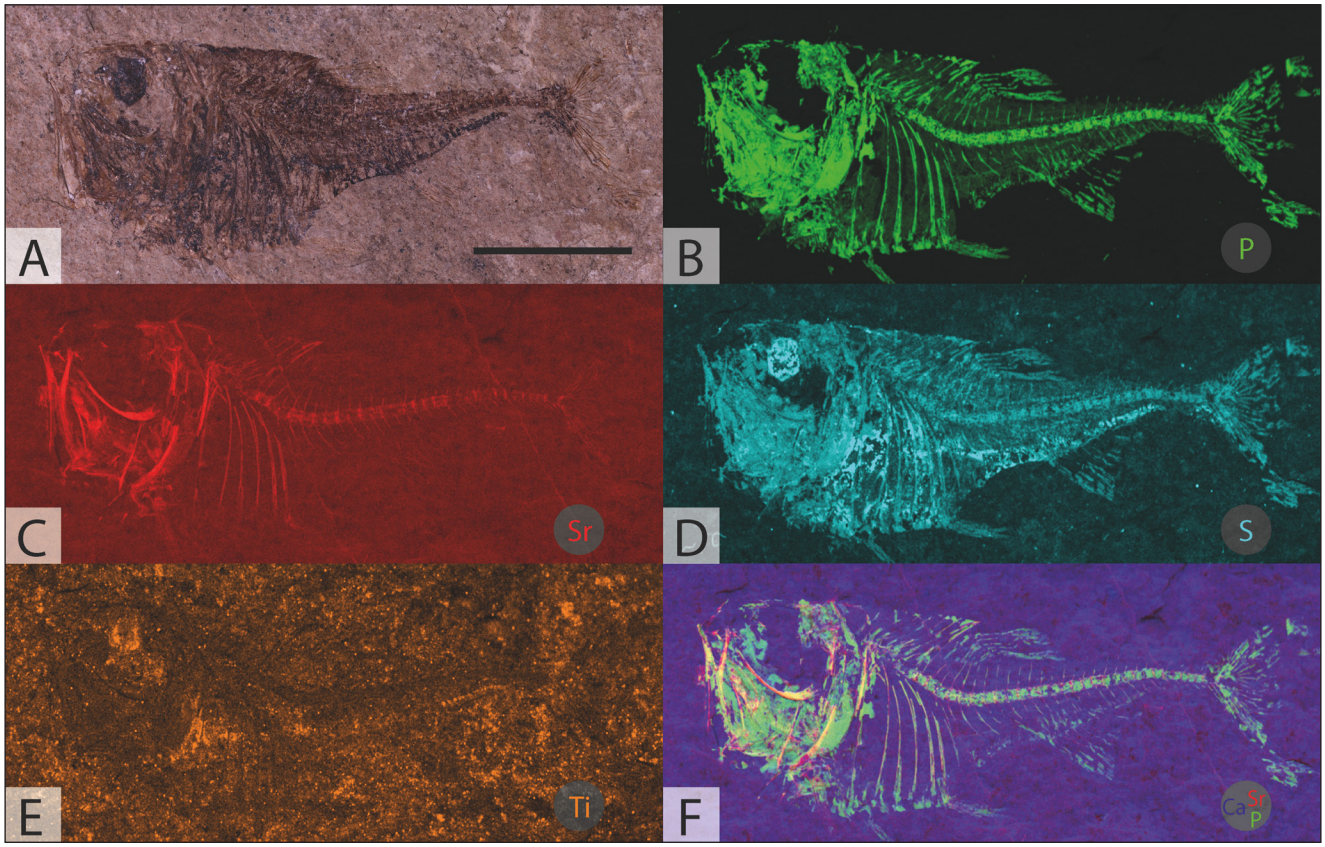

Fig. 16 - †*Argyropelecus zagrosensis* n. sp., paratype,IUGM 100892, from the Eocene of Babaheydar. A) high-resolution photo image; B) phosphorous element map; C) strontium element map; D) sulphur element map; E) titanium element map; F) combined element map of strontium (red) phosphorous (green) and calcium (blue). Scale bar equals 10 mm.

Holotype: IUGM 100893, a nearly complete articulated skeleton, in part and counterpart, 31.6 mm SL (Fig. 15).

Paratype: IUGM 100892, a nearly complete articulated skeleton, 29.8 mm SL (Fig. 16).

Horizon and Locality: Pabdeh Formation, Upper Eocene; Babaheydar, Zagros Basin, Iran.

Measurements (as % SL)**:** Total length: 124.0; head length: 29.9–32.8; head depth: 35.5–37; snout length: 2.6; orbit diameter: 11.9–15.4; maximum body depth: 43.1–43.3; caudal peduncle length: 13.8–17; caudal peduncle depth: 5.9–7.3; predorsal length: 48.0–50.7; preanal length: 63.3–66.8; prepectoral length: 23.9–29.2; prepelvic length: 48.7; dorsal-fin base length: 8.1–8.8; anal-fin base length: 14.0–20.1 (Table 1).

Description

The body (Figures 15, 16, 17) is laterally compressed with a moderately deep prepelvic region; the postpelvic region is narrower and elongate, representing about 1.5 times the length of the prepelvic region. Overall, the head bones are moderately thick and less ossified than those of the other *Argyropelecus* species (see Baird 1971, Weitzman 1974). The mouth is large with a strongly oblique gape. The orbit is large and the distribution of the preserved pigment of the eyeball suggests that the eyes were telescopic in origin with dorsally oriented lenses (see Figs. 15E, 15L and 15D). The caudal peduncle is elongate and slender, and the caudal fin is forked with elongate lobes. The anal fin originates behind the posterior end of the dorsal fin.

The head is contained about 3.3 times in SL. The overall structure of the head skeleton (Fig. 18), coupled with the subhorizontal dorsal profile of the neurocranium, is indicative of a certain degree of morphological similarity with the extant species *Argyropelecus affinis* and *A. gigas*. The ethmoid region is inadequately preserved. The vomer is scarcely recognizable in the holotype. The frontals are the largest bones of the skull roof and form the dorsal margin of the orbit; they taper anteriorly, becoming expanded posteriorly showing a frontal crest only weakly ornamented with ridges, some of which continue posteriorly on the parietals. The parietals are robust and subrectangular in shape, bearing a small crest connected with the frontal one. The pterosphenoid is elongated, narrow, gently curved, similar to that of †*A. logearti*, and forms part of the posterior wall of the orbit (Carnevale 2003). The sphenotic is subtriangular, vertically oriented and

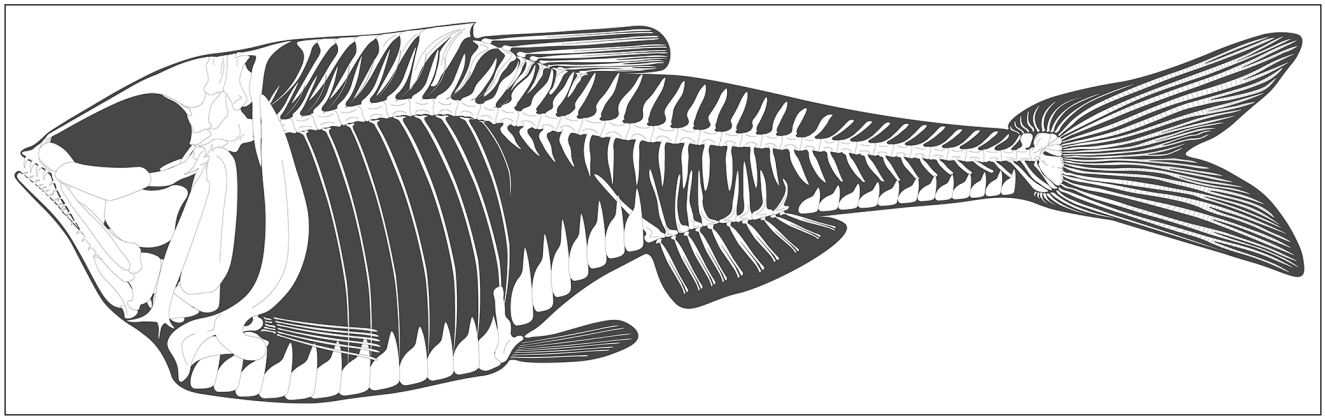

Fig. 17 - Interpretative reconstruction of the whole skeleton of †*Argyropelecus zagrosensis* n. sp. from the Eocene of Babaheydar, based on IUGM 100892 and IUGM 100893.

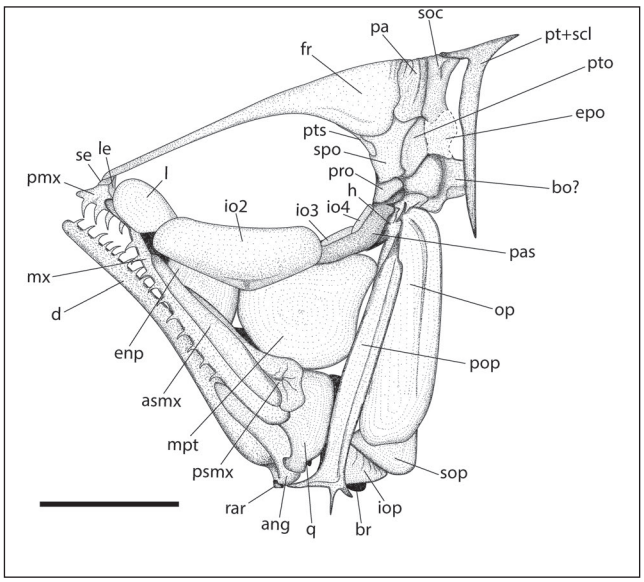

Fig. 18 - Interpretative reconstruction of the head of †*Argyropelecus zagrosensis* n. sp. from the Eocene of Babaheydar, based on IUGM 100892 and IUGM 100893. Abbreviations: ang: angular, asmx: anterior supramaxilla, bo: basioccipital, br: branchiostegal ray, d: dentary, enp: endopterygoid, epo: epioccipital, l: lachrymal, fr: frontal, h: hyomandibular, io: infraorbital bones, iop: interopercle, le: lateral ethmoid, mtp: metaptererygoid, mx: maxilla, op: opercle, pa: parietal, pas: parasphenoid, pmx: premaxilla, pop: preopercle, pt+scl: posttemporal+supracleithrum, pro: prootic, psmx: posterior supramaxilla, pto: pterotic, pts: pterosphenoid, q: quadrate, rar: retroarticular, se: supraethmoid, soc: supraoccipital, spo: sphenotic, sop: subopercle. Scale bar equals 10 mm.

notably large; this bone articulates anteromedially with the pterosphenoid, dorsally with the frontal and parietal, posteriorly with the pterotic, and ventrally mainly with the prootic. The otic and occipital portions of the neurocranium are consistent with those of the other *Agyropelecus* species. The long parasphenoid is thin anteriorly, becoming thick and strongly arched posteriorly, bearing an unpitted median keel-like structure.

The lachrymal is wide, subcircular in shape, while the second infraorbital is subtriangular. What appear to be the third and fourth infraorbital bones can be observed behind the second infraorbital; these are rod-like, remarkably smaller than the first two elements of the series.

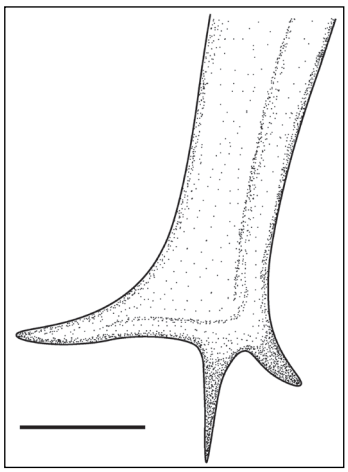

Fig. 19 - Interpretative reconstruction of the distal portion of the preopercular bone of †*Argyropelecus zagrosensis* n. sp. from the Eocene of Babaheydar, based on IUGM 100892 and IUGM 100893. Scale bar equals 2 mm.

The premaxilla is short and bears a well-developed ascending process. The maxilla is elongated and gently curved, extending posteroventrally up to the posterior half of the orbit. Premaxillary and maxillary teeth are not fully preserved but their overall shape and arrangement resemble those of †*A. iranicus*. There are two supramaxillae; the anterior one is the largest, it is elongated and covers most of the dorsal margin of the maxilla; the posterior supramaxilla is not preserved in the holotype and is barely visible in the paratype, being apparently similar to that of other congenerics, as described by Weitzman (1974).The lower jaw is elongated, triangular in shape, and does not extend significantly beyond the premaxilla. The dentary is slender and less obliquely oriented compared to that of †*A. iranicus*; its ventral margin is slightly concave. Dentary teeth are small, similar to those of the upper jaw.

The quadrate is large, well-ossified and subtriangular in outline, with a gently curved posterior margin. Most of the bones of the suspensorium are only moderately preserved. The metapterygoid, the largest bone of the suspensorium, is well-ossified and subquadrangular in shape. The endopterygoid is elongated and subtriangular in outline. The ectopterygoid and palatine are difficult to recognize. The hyomandibula is narrow and occupies about two-thirds of the head depth. The presence of the hyomandibular spine cannot be determined due to coverage by other bones.

The opercular series is poorly preserved in the holotype but its elements can be partially recognized in the paratype. The preopercle (Figs. 18–19) is L-shaped with a very short anterior arm as in other *Argyropelecus* species; a long vertically directed spine is present, along with a smaller posterior almost horizontal posteriorly directed spine (Fig. 19). The opercle is subquadrangular in shape and vertically developed; its anterior margin is straight, while the posterior one is gently convex.

The hyoid apparatus is difficult to describe since most of its elements are preserved as feeble impressions. The anterior ceratohyal is robust and elongated, exhibiting a concave ventral margin, supporting at least five branchiostegal rays. Although the morphology of the posterior ceratohyal cannot be properly determined, it seems to bear three plate-like branchiostegal rays. The urohyal is bifurcated distally.

The vertebral column consists of 38 vertebrae (15+23), like *Argyropelecus hemigymnus, A. olfersii, A. affinis, A. gigas,* and the fossil species †*A. logearti* and †*A. bullockii*. The abdominal region exhibits a slight kyphotic curve, while the caudal region appears to be more linear. The vertebral centra are subquadrangular, decreasing in size posteriorly. The neural spines of the anterior abdominal vertebrae are thin and gently curved. The neural and haemal spines of the anterior caudal vertebrae are subvertical and narrow, not expanded, and spatulate as in †*A. iranicus*. The neural spines of the vertebrae of the caudal peduncle are gradually shortened backward and obliquely oriented, like their opposite haemal spines. Like in the extant species of the '*Argyropelecus affinis* complex', the haemal spines involved in the anal-fin hiatus are not heavily modified (see Harold 1993). The posterior four abdominal vertebrae bear short and thick parapophyses. There are nine pairs of ribs, eight of which are enlarged and extend to the ventral margin of the body; the last rib is thin and short and is located behind the pelvic girdle. At least six pairs of delicate epineurals can be observed associated with the abdominal vertebrae.

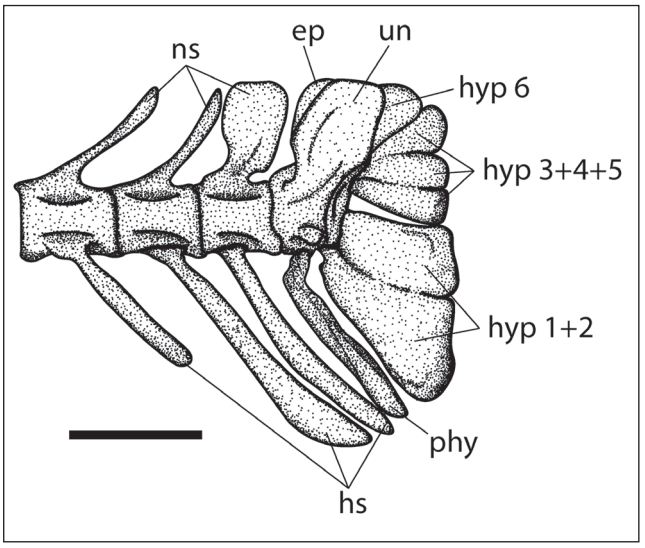

Fig. 20 - Interpretative reconstruction of the caudal skeleton of †*Argyropelecus zagrosensis* n. sp. from the Eocene of Babaheydar, based on IUGM 100892 and IUGM 100893. Abbreviations: ep: epural, hyp: hypural, hs: haemal spine, ns: neural spine, phy: parahypural, un: uroneural. Scale bar equals 5 mm.

The caudal fin (Fig. 20) is distinctly long and forked and comprises 19 (9+10) principal rays, plus at least nine upper and seven lower procurrent rays. Although the caudal skeleton is not perfectly preserved in either of the available specimens, it appears to be well-ossified, resembling the condition of the other *Argyropelecus* species (see Weitzman 1974). The compound centrum is ostensibly formed by the fusion of the first preural and two ural centra. The first and second hypurals are fused to each other, at least proximally, into a subtriangular plate, as are the third, fourth and fifth hypurals, whereas the sixth hypural is separated from the others. Overall, the caudal skeleton is very similar to that of †*Argyropelecus iranicus, A. aculeatus*, †*A. logearti, A. hemigymnus, A. lychnus, A. olfersii* and *A. sladeni* (see Baird 1971; Weitzman 1974; Carnevale 2003). There is a single subquadrangular, plate-like uroneural fused to the compound centrum. A plate-like epural is present between the neural spine of the second preural centrum and the sixth hypural. The parhypural is autogenous and lacks a parhypurapophysis. Additionally, the haemal spines of the second and third preural vertebrae are elongated and appear to be autogenous.

The dorsal fin is preceded by eight supraneurals, the first of which inserts in the first interneu-

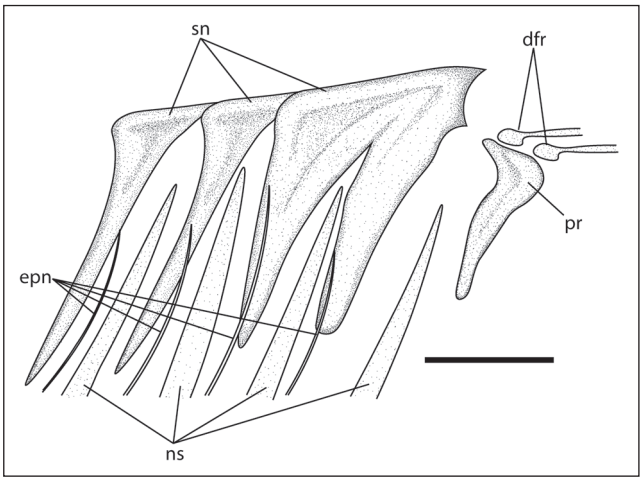

Fig. 21 - Interpretative reconstruction of the dorsal blade skeleton of †*Argyropelecus zagrosensis* n. sp. from the Eocene of Babaheydar, based on IUGM 100892 and IUGM 100893. Abbreviations: dfr: dorsal fin ray, epn: epineural, ns: neural spine, pr: dorsal-fin pterygiophores, sn: supraneural. Scale bar equals 5 mm.

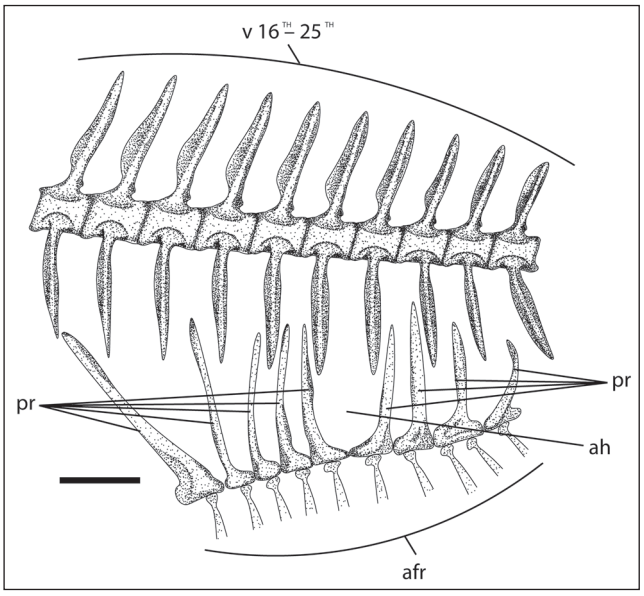

Fig. 22 - Interpretative reconstruction of the postabdominal region and anal-fin region, showing the modified structure hosting the anal hiatus of †*Argyropelecus zagrosensis* n. sp. from the Eocene of Babaheydar, based on IUGM 100892 and IUGM 100893. Abbreviations: afr: anal fin rays, ah: anal hiatus, pr: anal-fin pterygiophores, v: vertebrae. Scale bar equals 5 mm.

ral space (Fig. 21). The first supraneural is notably curved whereas the other ones are straight. Each supraneural has an expanded distal head whose anterior and posterior tips are associated with those of the adjacent elements forming collectively a robust dorsal blade. The seventh and eighth supraneurals are fused distally, forming the apex of the dorsal blade, which does not protrude significantly from the dorsal margin of the body. The dorsal fin has a short base and inserts in the first half of the body; there are eight distally bifurcate dorsal-fin rays supported by seven pterygiophores; the first dorsal-fin ray is in supernumerary association on the first dorsal-fin pterygiophore.

The anal fin originates behind the posterior end of the dorsal-fin base. The anal fin comprises ten distally bifurcated rays, supported by nine pterygiophores; the first anal-fin rays is supernumerary on the first pterygiophore. The first pterygiophore is greatly elongated and thin, obliquely inclined. The anal hiatus (Fig. 22) lies between the seventh and eighth pterygiophores and resembles that of the species of the '*A. affinis* complex' (see Baird 1971, fig. 15).

The pectoral girdle is well-ossified and robust, apparently lacking any ornamentation. The posttemporal plus supracleithrum are broad with an inverted L-shape. The cleithrum is sigmoid in shape, characterized by a remarkably large ascending arm. The ventral portion of the cleithrum is thick, terminating distally into a ventrally oriented thick spine. The coracoid is broad distally and constricted in the middle, being almost hourglass-shaped. The scapula is poorly preserved. The pectoral-fin radials are not preserved, and at least four long and pectoral-fin rays are recognizable, although their number was certainly higher in origin.

The pelvic girdle (Fig. 23) and fins are located below the dorsal-fin base. The basipterygium is slender and vertically oriented, articulated with the seventh and eighth ribs. The ischiatic process is vertical, while the iliac process is small and lacks any distinct spine, serration or other ornamentation, resembling the con-

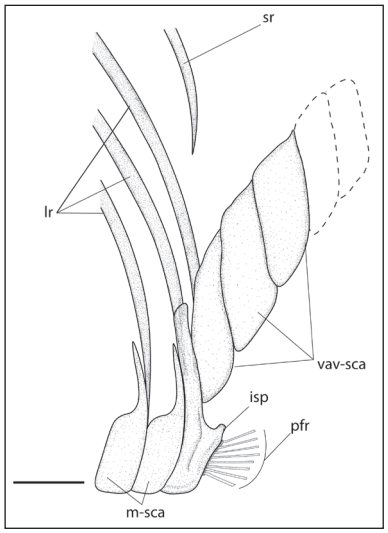

Fig. 23 - Interpretative reconstruction of the pelvic girdle of †*Argyropelecus zagrosensis* n. sp. from the Eocene of Babaheydar, based on IUGM 100892 and IUGM 100893. Abbreviations: isp: ischial process, lr: elongate ribs, m-sca: modified scales, pfr: pelvic-fin rays, sr: short ribs, vav-sca: VAV scales. Scale bar equals 5 mm.

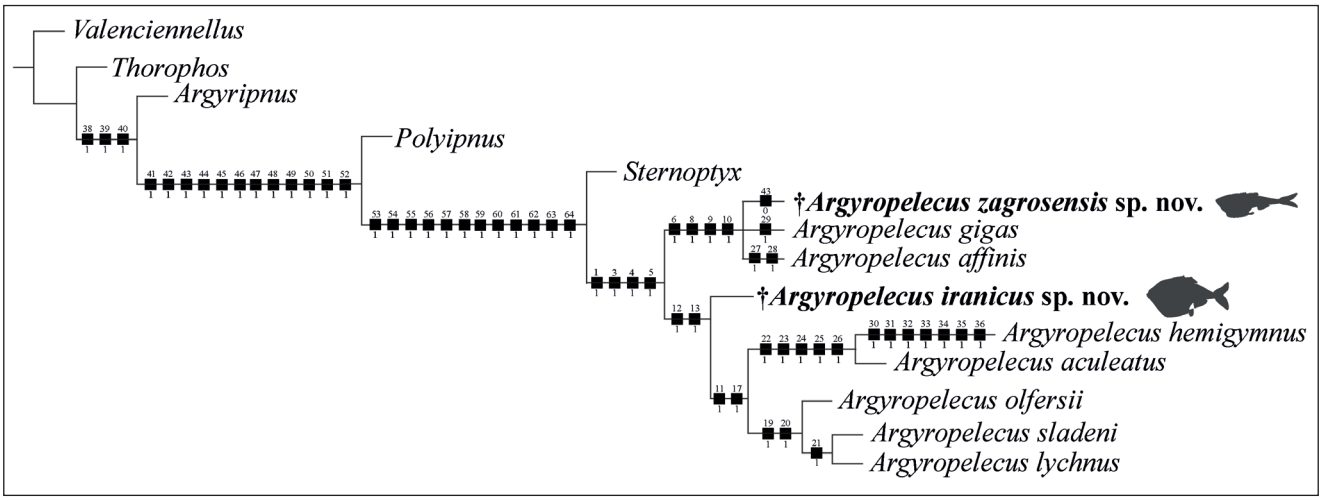

Fig. 24 - The tree retrieved in TNT based upon 64 characters and 14 taxa, showing the hypothetical phylogenetic relationship of †*Argyropelecus iranicus* and †*Argyropelecus zagrosensis* within the Sternoptichidae. Synapomorphies supporting the clades are indicated as nodes represented by black squares whose character numbers and states are placed above and below the node, respectively.

dition observed in *A. affinis* and *A. gigas* (see Baird 1971; Harold 1993). The angle between the ischiatic and pubic processes is broad, measuring approximately 60 degrees. The pelvic fin consists of at least five slender fin rays. There is no evidence of postabdominal spines, a feature not observed in any other species of the genus *Argyropelecus*.

There are no body scales, except for the highly modified stiff bony scales at the ventral body margin, forming a ventral keel extending from the anterior tip of the coracoid to the anal fin, which supported the ventral photophores. There are scales between the pelvic and anal fins (VAV photophores scales; see Weitzman 1974), which are longer than those of the prepelvic scales. There are traces of a horizontal discontinuous organic band that document the original presence of hypaxial photophore groups (BR, IP, OV, VAV, AC), as well as of the OP photophores (see Figs. 15D –E, K, L and 16D–E).

Phylogenetic analysis

The analysis of 64 morphological characters coded for 14 taxa yielded a single tree (Fig. 24), having a tree length of 40 steps, CI of 0.941 and RI of 0.972. The high consistency and retention indices suggest that the level of homoplasy is very low and that, once evolved, most characters are retained along branches and character reversal events are relatively uncommon. The resulting tree closely resembles the cladogram presented by Harold (1994, Fig. 1), from which the character matrix was taken. This cladogram originally included only the extant species of *Argyropelecus*.

The tree is almost completely resolved, with the genus *Argyropelecus* and the subfamily Sternoptychinae representing monophyletic groups. In our tree topology, *Thorophos, Argyripnus*, *Polyipnus* and *Sternoptyx* are successive sister taxa to the genus *Argyropelecus*. The monophyly of the clade composed by *Argyripnus* plus the Sternoptychinae (*Polyipnus* + (*Sternoptyx* + *Argyropelecus*) is supported herein by three characters: presence of an anal hiatus (ch. 38 [1]); presence of the lateral processes in the rostrodermethmoid (ch. 39 [1]); presence of 10 PV photophores in post-larvae or adult fishes (ch. 40 [1]).

The monophyly of the subfamily Sternoptychinae is supported by 12 characters: body deep, with maximum body depth comprised between 50 and 125% of SL (ch. 41 [1]); presence of the preopercular spine (ch. 42 [1]); presence of at least one iliac spine in the pelvic girdle (ch. 43 [1]); presence of abdominal keel, composed by stiff bony scales (ch. 44 [1]); length of the posterior ceratohyal more than 50% of that of the anterior ceratohyal (ch. 45 [1]); posterior end of the anterior ceratohyal larger than the anterior tip (ch. 46 [1]); pelvic girdle with the surface turned medially and pressed against its fellow of the opposite side (ch. 47 [1]); pelvic girdle vertically disposed, bound by ligaments to the posterior ribs (ch. 48 [1]); presence of bony ridges or crest on parietals in continuity with frontals (ch. 49 [1]); presence of enlarged and thick ribs (ch. 50

[1]); symplectic club-shaped and thick (ch. 51 [1]); enlarged exoccipital pedicles (ch. 52 [1]).

The sister group relationship between *Sternoptyx* and *Argyropelecus* is supported by 12 characters: presence of pits, ridges, and ornamentation on neurocranial bones or pectoral girdle or both (ch. 53 [1]); small-sized saccular otoliths (ch. 54 [1]); rostrum of the saccular otolith very reduced (ch. 55 [1]); endopterygoid short (ch. 56 [1]); ectopterygoid elongate and slender (ch. 57 [1]); coronoid process of the dentary absent (ch. 58 [1]); dorsal limb of preopercle and hyomandibula elongate (ch. 59 [1]); dorsal border of the quadrate articulating with metapterygoid (ch. 60 [1]); ventral border of the parasphenoid strongly convex (ch. 61 [1]); maxilla slender and straight (ch. 62 [1]); more than six rib-bearing vertebrae (ch. 63 [1]); urohyal deeply incised (ch. 64 [1]).

The monophyly of the genus *Argyropelecus* is supported by four characters: ossification of the ventral limb of the posttemporal incomplete or restricted (ch. 1 [1]); presence of a ventral, unpitted median keel-like structure on the parasphenoid that extends posteriorly beyond the point of dorsal inflection (ch. 3 [1]); longitudinal parietal crest turning medially in a smooth arc (ch. 4 [1]); 12 PV photophores in the abdominal keel present (ch. 5 [1]).

The *Argyropelecus* clade shows a distinct dichotomy formed by the lineage of low-bodied species (†*A. zagrosensis* n. sp., *A. gigas*, and *A. affinis*) sister to the clade including the deep-bodied species (†*A. iranicus* n. sp., *A. hemigymnus, A. aculeatus, A. olfersii, A. sladeni, A. lychnus*). The low-bodied species are in a polytomous relationship that is supported by four characters: first and second hypurals completely fused, forming a hypaxial hypural plate (ch. 6 [1]); lateral process of the infrapharyngobranchial of the third gill arch extending to the cartilaginous tip (ch. 8 [1]); ischial and pubic processes of each side of the pelvic girdle separated by a broad angle of about 60° (ch. 9 [1]); and widely spaced posterior IC photophores (VAV and AC) (ch. 10 [1]). *A. gigas* is distinguished by a single autapomorphy (long and straight second gill arch; ch. 29 [1]), whereas *A. affinis* exhibits two autapomorphies: anterodorsal surface of the ventral part of the cleithrum produced into an acute spine-like angle (ch. 27 [1]); and pits on the medial and dorsal surfaces of the anteroventral section of the cleithrum present (ch. 28 [1]). †*A. zagrosensis* n. sp. shows a single autapomorphy, namely the absence of the iliac spines in the pelvic girdle (ch. 43 [0]).

The position of †*A. iranicus* n. sp. as a sister taxon to the clade composed of all extant deep-bodied *Argyropelecus* is supported by two characters: neural and haemal spines in the median region very expanded and spatulate (ch. 12 [1]); seventh and eighth pterygiophores of the anal fin extremely modified to accommodate the anal hiatus (ch. 13 [1]). The extant deep-bodied *Argyropelecus* species are united by two characters: presence of a dorsally directed "spine" on the posterodorsal margin of the parhypural (ch. 11 [1]); and presence of a blade-like process extending anteriorly to the iliac spine, triangular in shape and aligned with the modified scales (ch. 17 [1]).

The position of *A. hemigymnus* as a sister taxon to *A. aculeatus* is supported by five characters: tip of the dorsal blade expanded and high, largely protruding from the dorsal margin of body (ch. 22 [1]); shafts of the seventh and eighth supraneurals fused only for the distal third of their length (ch. 23 [1]); presence of lateral wing-like processes on the posterior process of the dorsal blade (ch. 24 [1]); anterior margin of the tenth neural spine tightly bound by connective tissue to the expanded neural spine immediately anterior (ch. 25 [1]); and dorsal process of the second hypobranchial located posteriorly (ch. 26 [1]).

The position of *A. olfersii* as a sister taxon to the clade composed by *A. sladeni* plus *A. lychnus* is supported by two characters: triangular posterior process of the dorsal blade elongate, contacting the anterior region of the dorsal fin (ch. 19 [1]); teeth of the fused tooth plate of the fifth ceratobranchial placed only in the very proximal end (ch. 20 [1]).

Finally, the position of *A. sladeni* as sister to *A. lychnus* is supported by a single trait: shape of the third infrapharyngobranchial straight and not greatly expanded at either ends (ch. 21 [1]).

Geometric morphometric analysis

The Relative Warp analysis identified 96 axes (RWs), with the first three together accounting for 90.24% of the total morphological variability. A scree-plot (Fig. 25) was used to visualize the variability explained by each RW axis, showing that only the first three axes explain over 5% of the variation. Morphological variation among taxa was examined by analyzing the distribution of genera within the

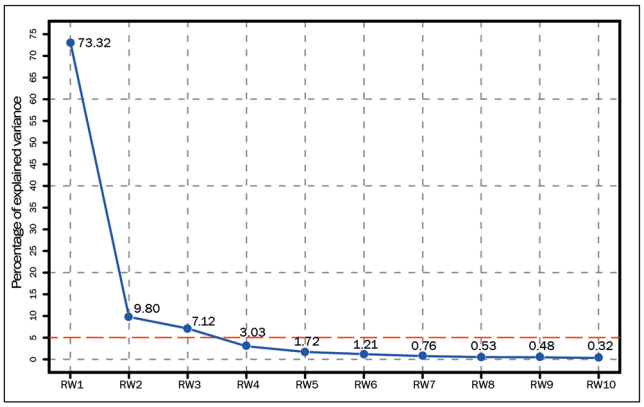

Fig. 25 - Scree-plot of the first ten RW components illustrating the percentage of explained variance of each axis.

morphospace defined by these three axes. Consensus shape and vectors of relative landmark displacement showing shape changes from the consensus shape are reported in Figure 26.

The first RW axis describes the elongation of the body and represents the contrast between deep-bodied and slender shapes (Fig. 27). Extreme negative RW1 values are occupied by genera such as *Danaphos* and *Sonoda*, characterized by slender bodies with no abdominal keel; conversely, in positive values lie deep-bodied genera having prominent abdominal keel (e.g., *Sternoptyx*). RW2 explains the variation in the relative position of the tip of the dorsal blade and of the pelvic girdle, as well as the relative position of the caudal fin in relation to the first vertebrae (Fig. 27). The genus *Sternoptyx* (lying in positive RW2 values) has a dorsal-blade tip aligned with the pelvic girdle conversely, most specimens of the genus *Argyropelecus* (particularly those of the '*lychnus* complex') and *Maurolicus*, which lie on negative RW2 values, have a dorsal-blade tip anterior to the pelvic girdle. RW3 explains how the abdominal keel is marked in relation to the postabdominal region. (Fig. 28).Taxa lying at positive RW3 values (e.g., *Maurolicus* and most *Polypnus* specimens) show a more ovoid body, with the caudal region that tapers gradually and more posteriorly, whereas negative values are occupied by taxa with a marked difference in depth between the abdominal and caudal region, with this latter steeply tapering at the anal-fin origin (e.g., *Danaphos*).

The morphospace occupation shows that the genera are well separated from each other, with only *Polyipnus* that partially overlaps the convex hulls of *Argyropelecus*, indicating that some taxa of both genera show similar overall body physiognomy. As far as the genus *Argyropelecus* is concerned, the convex hulls of the '*A. affinis* complex' (including †*A. zagrosensis*) and '*A. lychnus* complex' (including †*A. iranicus*) are completely separated in the plot formed by the first two RW axes, whereas they show partial overlap in the morphospace built on RW1 and RW3, suggesting that the two complexes differ considerably in the overall body physiognomy. Noteworthy, †*A. zagrosensis* n. sp. occupies the extreme periphery of the morphospace on negative values of RW1, resulting in a considerable contribution to the overall disparity of the genus.

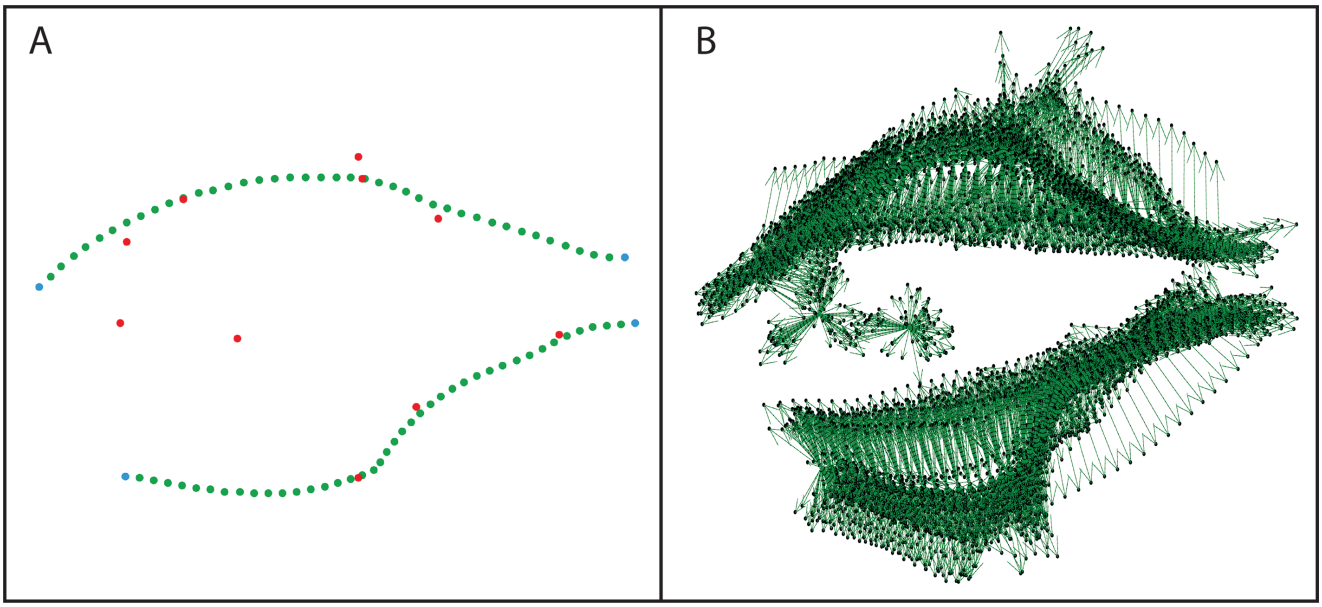

Fig. 26 - A) Consensus shape. B) Vectors of relative landmark displacement showing shape changes from the consensus shape.

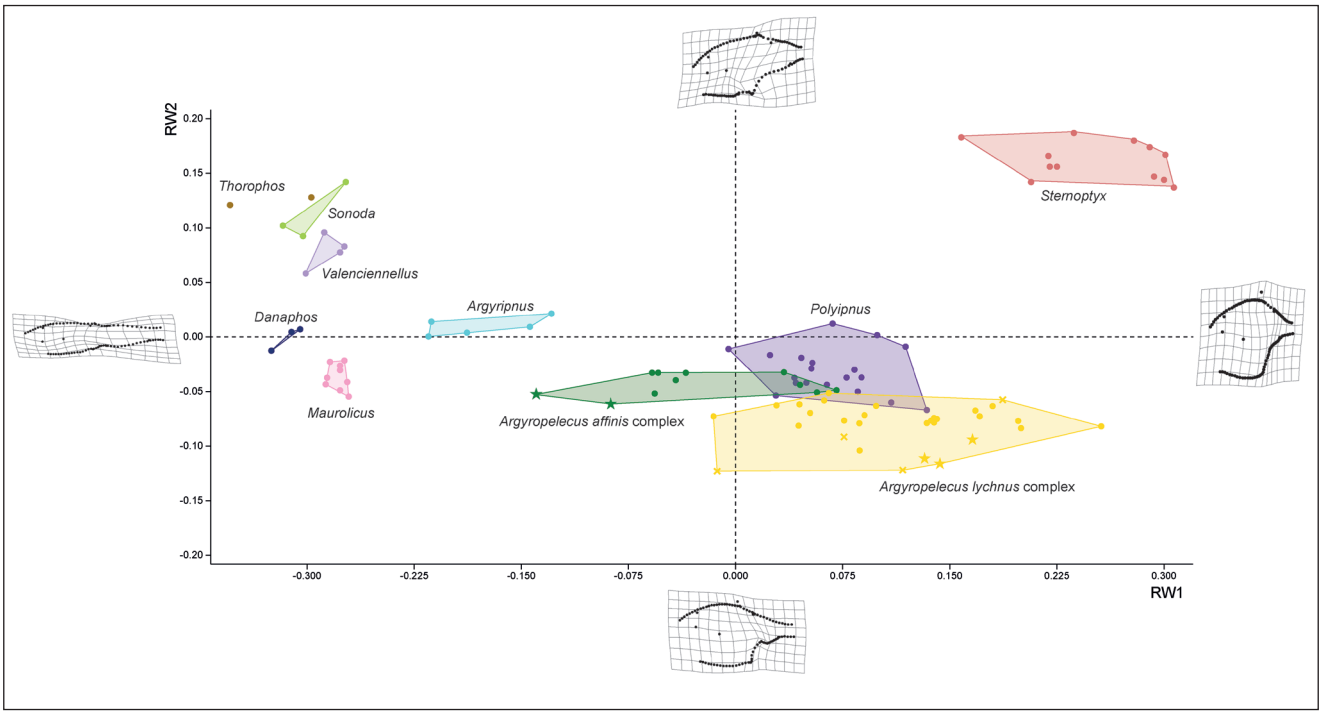

Fig. 27 - Morphospace plotted on the first two RW axes. Deformation grid plots illustrate the shapes lying at extreme values along each RW axis. Full dots represent extant taxa, "x" indicate fossil taxa and stars mark the position of the new fossils †*A. iranicus* n. sp. and †*A. zagrosensis* n. sp.

The quantitative morphospace occupation of the Sternoptychidae is also supported by the non-parametric tests PERMANOVA and ANOSIM (Tables 2 and 3), both of which indicate that '*A. affinis* complex' and '*A. lychnus* complex' significantly occupy different regions of the morphospace relative to each other and the other genera ($p < 0.05$).

The Partial Least Square analysis (PLS) revealed a moderate and significant positive correla-

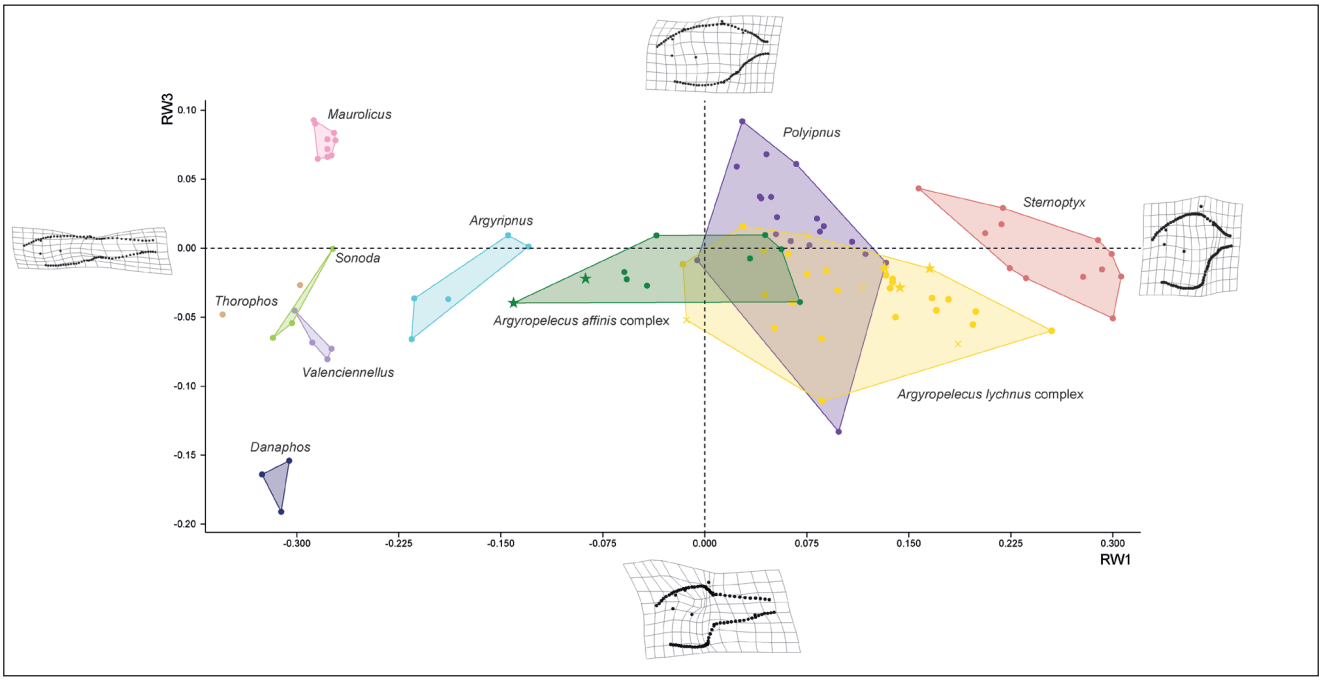

Fig. 28 - Morphospace plotted on the first and the third RW axes. Deformation grid plots illustrate the shapes lying at extreme values along each RW axis. Full dots represent extant taxa, "x" indicate fossil taxa and stars mark the position of the new fossils †*A. iranicus* n. sp. and †*A. zagrosensis* n. sp.

	Argyripnus	*A. affinis* complex	*A. lychnus* complex	*Polyipnus*	*Sternoptyx*	*Danaphos*	*Maurolicus*	*Sonoda*	*Thorophos*	*Valenciennellus*
Argyripnus		94.86	23.27	146.90	313.40	30.00	59.64	31.35	30.56	32.76
A. affinis complex	0.0001		31.17	15.40	166.60	120.60	298.70	129.70	98.82	156.10
A. lychnus complex	0.0006	0.0002		18.66	175.10	49.25	115.70	54.51	43.62	63.42
Polyipnus	0.0002	0.0001	0.0003		262.50	249.10	604.90	246.40	194.40	303.50
Sternoptyx	0.0003	0.0001	0.0001	0.0001		371.70	1043.00	306.60	227.60	416.20
Danaphos	0.0173	0.0003	0.0031	0.0012	0.0025		31.38	27.39	27.13	37.36
Maurolicus	0.0008	0.0001	0.0001	0.0001	0.0001	0.0049		133.50	136.20	157.20
Sonoda	0.0185	0.0004	0.0042	0.0005	0.0025	0.0997	0.0046		0.83	3.08
Thorophos	0.0480	0.0024	0.0152	0.0034	0.0105	0.0988	0.0187	0.5974		7.05
Valenciennellus	0.0082	0.0001	0.0011	0.0002	0.0008	0.0302	0.0016	0.0548	0.0646	

Tab. 2 - PERMANOVA nonparametric tests used to assess significant differences in morphospace occupation between the 10 groups; *p*-values are in white cells on the down/left side of the matrix, *F*-values are in grey cells, on the up/right side of the matrix.

	Argyripnus	*A. affinis* complex	*A. lychnus* complex	*Polyipnus*	*Sternoptyx*	*Danaphos*	*Maurolicus*	*Sonoda*	*Thorophos*	*Valenciennellus*
Argyripnus		0.9892	0.7236	0.9998	1.0000	1.0000	0.9662	1.0000	1.0000	1.0000
A. affinis complex	0.0001		0.5047	0.2746	0.9964	1.0000	0.9998	1.0000	1.0000	1.0000
A. lychnus complex	0.0003	0.0001		0.3838	1.0000	0.9889	0.9811	1.0000	1.0000	0.9931
Polyipnus	0.0001	0.0002	0.0011		1.0000	1.0000	1.0000	1.0000	1.0000	1.0000
Sternoptyx	0.0003	0.0001	0.0001	0.0001		1.0000	1.0000	1.0000	1.0000	1.0000
Danaphos	0.0177	0.0004	0.0050	0.0011	0.0025		1.0000	1.0000	1.0000	1.0000
Maurolicus	0.0007	0.0001	0.0001	0.0001	0.0001	0.0037		1.0000	1.0000	1.0000
Sonoda	0.0202	0.0002	0.0032	0.0006	0.0017	0.0974	0.0061		-0.0833	0.3333
Thorophos	0.0479	0.0019	0.0172	0.0055	0.0098	0.0908	0.0168	0.7003		0.8214
Valenciennellus	0.0064	0.0002	0.0006	0.0004	0.0007	0.0276	0.0009	0.0589	0.0681	

Tab. 3 - ANOSIM nonparametric tests used to assess significant differences in morphospace occupation between the 10 groups; *P*-values are in white cells on the down/left side of the matrix, *R*-values are in grey cells, on the up/right side of the matrix.

tion between body shape and vertical distribution ($r = 0.54$; $p < 0.05$), suggesting that morphological differences might be related to vertical habitat partitioning in the water column (Fig. 29). In particular, elongate and tapered bodies with elongated postabdominal region, dorsal blade low or absent, and no abdominal keel are associated with shallow water taxa. Conversely, deep-bodied taxa having short

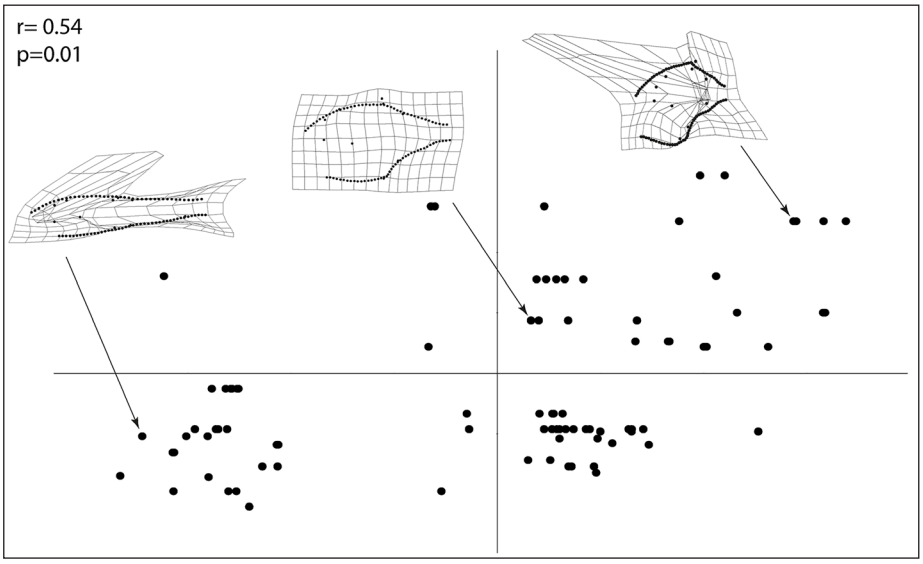

Fig. 29 - PLS analysis showing the correlation between morphometric variation and the maximum vertical distribution within the extant Sternoptychidae. The x-axis is related to the vertical distribution, with the negative values corresponding to the shallow water, whereas deep water corresponds to positive values. The minimum depth value is 200 m, while the maximum depth value is 2700 m. Significance of this correlation is shown by the *r* and *p*-values.

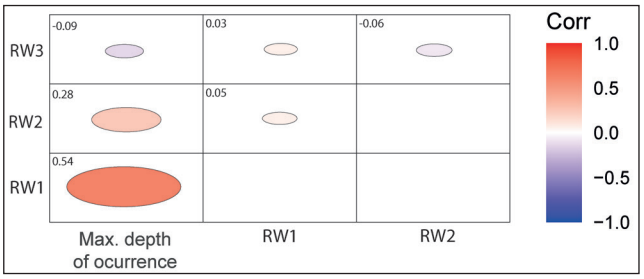

Fig. 30 - Collinearity analysis performed on the first three RW axes using the GEMMA toolbox for R (version 4.5.0) (Pilade et al. 2025).

postabdominal region, protruding dorsal blade, and distinct abdominal keel inhabit deeper waters. The collinearity analysis reveals that only the first axis (RW1) concurs to explain the correlation between shape and vertical distribution (Fig. 30).

Discussion

The morphological analysis of the new specimens described in this work reveals two distinct morphotypes exhibiting a variety of distinctive features that support their identification as new species of deep-sea hatchetfish, family Sternoptychidae. According to Weitzman (1974), the Sternoptychidae encompasses ten extant genera: *Araiophos*, *Argyripnus*, *Argyropelecus*, *Danaphos*, *Maurolicus*, *Polyipnus*, *Sonoda*, *Sternoptyx*, *Thorophos*, and *Valenciennellus* (Harold 1993). These genera share several synapomorphies, such as the presence of type alpha photophores arranged in glandular clusters, three branchiostegal rays articulated with the posterior ceratohyal, parietals separated by the supraoccipital, and absence of basihyal and endopterygoid teeth (Harold 1993). Harold & Weitzman (1996) recognized more than 20 characters supporting the monophyly of the Sternoptychidae in a subsequent phylogenetic analysis of stomiiform fishes. However, they also noted that only two of these characters are unique and unreversed: the separation of the parietals by the supraoccipital and the arrangement of the photophores in clusters, a result of their development by budding (see Ahlstrom et al. 1984). In our case, the presence of type alpha photophores associated with the modified scales of the ventral keel, the hypurals 1+2 fused, and the absence of endopterygoid teeth support the assignment of the material described in this work to the deep-sea hatchetfish family Sternoptychidae.

Within the family Sternopychidae, the Sternoptychinae is a monophyletic clade diagnosed by more than 30 synapomorphies (Baird 1971; Weitzman 1974; Harold 1993; Harold & Weitzman 1996), among which body depth more than 30% of SL, presence of a distinct abdominal keel, prominent frontal crest followed by the parietal crest, ribs enlarged and preopercular spines unquestionably support the assignment of †*A. iranicus* n. sp. and †*A. zagrosensis* n. sp. to the subfamily Sternoptychinae.

The genus *Argyropelecus* is supported by several synapomorphies exhibited by both †*A. iranicus* n. sp. and †*A. zagrosensis* n. sp., including the presence of a ventral, unpitted median keel-like structure on the parasphenoid that extends posteriorly beyond the point of dorsal inflection, and the presence of the modified scales of the abdominal keel that likely supported photophores in origin (Harold 1993). The morphospace analysis also suggests that these two species belong to the genus *Argyropelecus*; indeed, both species fall within the convex hull of this genus (divided into the two complexes in the analysis), proving that the body shapes of this genus have been maintained over time.

According to morphological observations and the phylogenetic analysis, †*Argyropelecus iranicus* n. sp. can be considered as the sister taxon of the extant species belonging to the '*A. lychnus* complex' (see Baird 1971; Harold 1993) since it exhibits some diagnostic traits of this group, including neural and haemal spines being very expanded and spatulate in the median region, shape of the dorsal blade, body depth, and the structure of the anal hiatus with greatly modified pterygiophores of the anal fin.

†*A. iranicus* n. sp. differs from the other deep-bodied *Argyropelecus* species in having a unique combination of meristic features. †*A. iranicus* n. sp. differs from *A. aculeatus* since the former has 15 abdominal vertebrae (vs. 11 in *A. aculeatus*), two short post-pelvic rib (vs. one in *A. aculeatus*), a single postabdominal (pelvic) spine (vs. two *A. aculeatus*), scarcely ornamented bones of the neurocranium (vs. heavily ornamented), moderately protruding dorsal blade (vs. remarkably protruding), ventral preopercular spine short and stout (vs. medium size, not particular stout), and posterior preopercular spine long and not curved (vs. medium size and curved) (see Baird 1971; Weitzman 1974; Harold 1993). †*A. iranicus* n. sp. differs from *A. olfersii* in several traits: a single postabdominal (pelvic) spine (vs.

two *A. olfersii*), absence of fang-like canines in the upper jaw (vs. present in *A. olfersii*), ventral preopercular spine short and stout (vs. long and anteriorly curved), and posterior preopercular spine long (vs. short and stout) (see Baird 1971; Weitzman 1974; Harold 1993). Two morphological features separate †*A. iranicus* from *A. sladeni*: a single postabdominal (pelvic) spine (vs. two *A. sladeni*), and the presence of a fang-like canine in the lower jaw (vs. absent in *A. sladeni*) (see Baird 1971; Weitzman 1974; Harold 1993).

†*A. iranicus* n. sp. differs from *A. lychnus* in the following morphological features: 15 abdominal vertebrae (vs. 11 in *A. lychnus*), two short postpelvic short ribs (vs. one in *A. lychnus*), three VAV photophore scales (vs. more than four *A. lychnus*), moderately ornamented frontals and other neurocranial bones (vs. extensively pitted), and ventral preopercular spine short and stout (vs. long) (see Baird 1971; Weitzman 1974; Harold 1993). †*A. iranicus* n. sp. differs from *A. hemigymnus* by having three VAV photophores scales (vs. four in *A. hemigymnus*), presence of a fang-like canine in the lower jaw (vs. absent in *A. hemigymnus*), dorsal blade moderately protruding from the dorsal margin of the body and subvertically oriented (vs. very protruding and vertically oriented), preopercular spines of different size (vs. both equal in size), ventral preopercular spine ventrally oriented (vs. serrated and backward oriented), and neural and haemal spines of the caudal vertebrae large and spatulate (vs. slender and thin) (see Baird 1971; Weitzman 1974; Harold 1993).

The comparison between †*A. iranicus* n. sp. and the three deep-bodied fossil taxa likely pertaining to the '*A. lychnus* species complex' is challenging, due to the limited information available for †*A. bullockii* and †*A. priscus* (see Cosmovici & Paucă 1943; David 1943; Baird 1971; Prokofiev 2002, 2005), whereas comparison with †*A. logearti* is more reliable thanks to the recent revision of this taxon (Carnevale 2003). †*A. iranicus* n. sp. differs from †*A. bullockii* in having a single postabdominal spine (vs. two in †*A. bullockii*), subvertically oriented dorsal blade (vs. vertically oriented) (David 1943). †*A. iranicus* n. sp. differs from †*A. priscus* in having a single postabdominal spine (vs. two in †*A. priscus*), moderately ornamented frontals and other head bones (vs. heavily pitted), and posterior preopercular spine long (vs. moderate size) (Jerzmańska 1968; Gregorová 1993; Prokofiev 2002, 2005). Finally, †*A. iranicus* n. sp. differs from †*A. logearti* by having 21 caudal vertebrae (vs. 26 in †*A. logearti*), three VAV photophore scales (vs. four), moderately ornamented frontals and other neurocranial bones (vs. heavily pitted), presence of a fang-like canine in the lower jaw (vs. absent), dorsal blade moderately protruding and subvertically oriented (vs. very protruding and vertically oriented), size of the preopercular spine, ventral preopercular spine ventrally oriented (vs. serrated and posteriorly oriented), and neural and haemal spines of the caudal vertebrae large and spatulate (vs. slender and much thin) (see Carnevale 2003).

Geometric morphometrics also strongly supports the inclusion of †*A. iranicus* n. sp. in the '*A. lychnus* complex': the new species, as well as all other fossil taxa known until today, belong to this morphotype characterized by a very deep body, a strongly protruding dorsal blade and a poorly developed postabdominal region.

The other species described herein, †*A. zagrosensis* n. sp., is aligned with the extant species of the '*A. affinis* species complex', which includes the extant species *A. affinis* and *A. gigas*. †*A. zagrosensis* n. sp. differs from *A. affinis* in having ornamentation on the frontals and other head bones highly reduced (vs. moderately ornamented in *A. affinis*), absence of iliac spines in the pelvic girdle (vs. 2 spines present) and absence of a fang-like canine on the lower jaw (vs. present), hypurals 1 and 2 fused (vs. not fused) (see Baird 1971; Weitzman 1974; Harold 1993). Finally, †*A. zagrosensis* n. sp. differs from *A. gigas* in having ornamentation on the frontals and other head bones (vs. moderately ornamented in *A. gigas*), absence of a fang-like canine on both the lower and upper jaw (vs. present in both jaws), dorsal blade scarcely-protruding and posteriorly oriented (vs. moderately protruding and subvertically oriented), hypurals 1and 2 fused (vs. not fused) and absence of iliac spines of the pelvic girdle (vs. 2) (see Baird 1971; Weitzman 1974; Harold 1993).

Investigation of morphospace occupation also supports the inclusion of †*A. zagrosensis* n. sp. in the '*A. affinis* complex' representing the first fossil species belonging to this morphotype. In addition, geometric morphometrics shows that †*A. zagrosensis* n. sp. is the most elongate and tapered among the species of the '*A. affinis* complex' and thus of the entire genus *Argyropelecus*. The study of the morphospace occupied by this genus strongly suggests that, like the genus *Polyipnus*, it includes a

high diversity of shapes; in particular, it is evident that the two complexes '*A. affinis*' and '*A. lychnus*' are well separated, where the main differences are related to body depth and elongation and to the caudal region.

The species of *Argyropelecus* described herein are relevant because they indicate that the three extant sternoptychine genera were already in existence in the Eocene and that the two morphological groups characteristic of the genus *Argyropelecus* have a deep origin, dating back to more than 40 Ma. Moreover, the morphometric analysis of the extant fishes in relation to their vertical distribution also suggests that elongated and tapered forms are associated with shallow depths, while the deep-bodied forms (species of the '*A. lychnus* complex') exhibit a much deep bathymetric range.

Conclusion

The new species †*Argyropelecus iranicus* n. sp. and †*Argyropelecus zagrosensis* n. sp. from the Eocene deposits of the Pabdeh Formation described herein shed new light on the early evolutionary history of the genus *Argyropelecus*. The well-preserved fossils documented in this study allowed for comprehensive analysis of their skeletal features also thanks to the μXRF elemental mapping. Both the phylogenetic analysis and the morphospace occupation analysis confirmed the presence of two distinct morphotypes within the genus *Argyropelecus*, among which the deep-bodied †*Argyropelecus iranicus* n. sp. pertains to the so-called '*A. lychnus* complex', whereas the more slender and elongate †*Argyropelecus zagrosensis* n. sp. belongs to the '*A. affinis* complex'.

Acknowledgements: Kristoffer Szilas is thanked for access to the μXRF facilities and machinery at the Department of Geosciences and Natural Resource Management, Copenhagen University. For reviewing the manuscript and providing many constructive suggestions for its improvement, we are particularly grateful to Ionut Grădianu and an anonymous reviewer. The research of AES was supported by the Carlsberg Foundation, grant no. CF23-1059. Research supported by grants (ex-60% 2024) to GC from the Università degli Studi di Torino.

Data Availability Statement

The data supporting the results of this research are available upon request. Interested researchers may contact the corresponding Author to obtain access.

References

Afsari S., Yazdi M., Bahrami A. & Carnevale G. (2014) - A new deep-sea hatchetfish (Teleostei: Stomiiformes: Sternoptychidae) from the Eocene of Ilam, Zagros Basin, Iran. *Bollettino della Società Paleontologica Italiana*, 53(1): 27-37.

Ahlstrom E.H., Richards W.J. & Weitzman S.H. (1984) - Families Gonostomatidae, Sternoptychidae, and associated stomiiform groups: development and relationships. In: Moser H.G., Richards W.J., Cohen D.M., Fahay M.P., Kendall Jr. A.W. & Richardson S.L. (Eds.) - Ontogeny and Systematics of Fishes. *American Society of Ichthyologists and Herpetologists*, Special Publication 1: 184-198.

Ala M.A., Kinghorn R.R.F. & Rahman M. (1980) - Organic geochemistry and source rock characteristics of the Zagros petroleum province, South West Iran. *Journal of Petroleum Geology*, 3: 61-89.

Anderson M.J. (2001) - A new method for non-parametric multivariate analysis of variance. *Austral Ecology*, 26(1): 32-46.

Arambourg C. (1929) - *Argyropelecus logearti*, un nouveau poisson bathypelagique du Sahelien. *Bulletin de la Société Géologique de France*, 29: 11-15.

Arambourg C. (1967) - Résultats Scientifiques de la Mission C. Arambourg en Syrie et en Iran (1938-1939). II. Les Poissons Oligocènes de l'Iran. *Notes et Mémoires sur le Moyen-Orient*, 8: 1-210.

Badcock J. (1984) - Sternoptychidae. In: Whitehead P.J.P., Bauchot M.-L., Hureau J.-C., Nielsen J. & Tortonese E. (Eds.) - Fishes of the North-eastern Atlantic and the Mediterranean: 302-317.

Baird R.C. (1971) - The systematics, distribution, and zoogeography of the marine hatchetfishes (family Sternoptychidae). *Bulletin of the Museum of Comparative Zoology*, 142: 1-128.

Baird R.C. (1986) - Tribe Sternoptychini. In Smith M.M. & Heemstra P.C. (Eds.) - Smiths' Sea Fishes: 255-259.

Baird R.C. & Eckardt M.J. (1972) - Divergence and relationship in deep-sea hatchetfishes (Sternoptychidae). *Systematic Zoology*, 21: 80-90.

Bannikov A.F. (2010) - Fossil acanthopterygian fishes (Teleostei, Acanthopterygii). In: Tatarinov L.P., Vorobyeva E.I., & Kurochkin E.N. - Fossil Vertebrates of Russia and Adjacent Countries. *GEOS:* 1- 244.

Bannikov A.F. (2018) - A new genus and species of stromateoid fishes (Perciformes, Stromateoidei) from the Lower Oligocene of the Northern Caucasus. *Paleontological Journal*, 52: 631-638.

Bannikov A.F. & Parin N.N. (1997) - The list of marine fishes from Cenozoic (Upper Paleocene-Middle Miocene) localities in southern European Russia and adjacent countries. *Journal of Ichthyology,* 37(2): 133-146.

Bannikov A.F. & Tyler J.C. (1995) - Phylogenetic revision of the fish families Luvaridae and Kushlukiidae (Acanthuroidei), with a new genus and two new species of Eocene luvarids. *Smithsonian Contributions to Paleobiology*, 81: 1-45.

Bannikov A.F., Tyler J.C. & Sorbini C. (2010) - Two new taxa of Eocene rabbitfishes (Perciformes, Siganidae) from the North Caucasus (Russia), with redescription of *Acanthopygaeus agassizi* (Eastman) from Monte Bolca (Italy) and a phylogenetic analysis of the family. *Bollettino del Museo Civico di Storia Naturale di Verona*, 34: 3-21.

Carnevale G. (2003) - Redescription and phylogenetic relationships of *Argyropelecus logearti* (Teleostei: Stomiiformes:

Sternoptychidae), with a brief review of fossil *Argyropelecus*. *Rivista Italiana di Paleontologia e Stratigrafia*, 109: 63-76.
Carnevale G. (2007) - Fossil fishes from the Serravallian (Middle Miocene) of Torricella Peligna, Italy. *Palaeontographia Italica*, 91: 3-69.
Carnevale G. (2008) - Miniature deep-sea hatchetfish (Teleostei: Stomiiformes) from the Miocene of Italy. *Geological Magazine*, 145: 73-84.
Carnevale G. & Tyler J.C. (2018) - The caudal skeleton of *Arambourgthurus scombrurus* (Arambourg, 1967), a Paleogene oceanic surgeonfish. *Proceedings of the Biological Society of Washington*, 131: 101-110.
Ciobanu M. (1977) - Fauna Fosila din Oligocenul de la Piatra Neamt. Editura Academiei Reoubiicii Socialiste Romania, Bucaresti.
Clarke K.R. (1993) - Non-parametric multivariate analysis of changes in community structure. *Austral Ecology*, 18(1): 117-143.
Cocco A. (1829) - Su di alcuni nuovi pesci de' mari di Messina. *Giornale di Scienze Lettere e Arti per la Sicilia*, 7(26): 138-147.
Cosmovici N.L. & Paucă M. (1943) - Ein neuer fossiler Fisch mit erhaltenen Leuchtorganen: *Argyropelecus cosmovicii* sowie Erwägungen zur Ablagerung der Menilitschiefer. *Bulletin de la Section Scientifique de l'Académie Roumaine*, 26: 271-280.
Coxall H.K. & Pearson P.N. (2006) - Taxonomy, biostratigraphy, and phylogeny of the Hantkeninidae (*Clavigerinella*, *Hantkenina*, and *Cribrohantkenina*). *Cushman Foundation Special Publication*, 41: 213-256.
Cushman J.A. (1925) - New foraminifera from the Upper Eocene of Mexico. *Contributions from the Cushman Foundation for Foraminiferal Research*, 1: 4-9.
Danil'chenko P.G. (1960) - Kost'istye ryby maikopskikh otlojeniy Kavkaza. *Dokl. Acad. Nawk SSSR*, 78: 28-32, Moscow.
Danilit'chenko P.G. (1962) - Fishes from the Dabakhanian Formation of Georgia. *Paleontologischeskii Zhurnal*, 1: 111-126.
Davesne D. (2017) - A fossil unicorn crestfish (Teleostei, Lampridiformes, Lophotidae) from the Eocene of Iran. *PeerJ*, 5:e3381.
David L.R. (1943) - Miocene fishes of southern California. *Geological Society of America, Special Paper*, 43: 1-181.
de Mecquenem R. (1908) - Note sur le Crétacé supérieur d'Husseinabad (Poucht-e-Kouh). In: Priem F. - Poissons fossiles de Perse. *Annales d'Histoire Naturelle*, *Paléontologie*, 1: 1-3.
Duméril A.M.C. (1805) - Zoologie analytique, ou méthode naturelle de classification des animaux, rendue plus facile à l'aide de tableaux synoptiques. i-xxxii + 1-344.
El-Sayed S., Friedman M., Anan T., Faris M. A. & Sallam H. (2021) - Diverse marine fish assemblages inhabited the paleotropics during the Paleocene-Eocene thermal maximum. *Geology*, 49(8): 993-998.
Fleisher R.L. (1974) - Cenozoic planktonic foraminifera and biostratigraphy, Arabian Sea, Deep Sea Drilling Project, Leg 23A. *Initial Reports of the Deep Sea Drilling Project*, 23: 1001-1072.
Froese R. & Pauly D. (2015) - FishBase (version 07/2015). World Wide Web electronic publication. Available at: www.fishbase.org
Garassino A., Bahrami A., Yazdi M. & Vega F.J. (2014) - Report on decapod crustaceans from the Eocene of Zagros Basin, Iran. *Neues Jahrbuch Für Geologie Und Paläontologie-Abhandlungen*, 274(1): 43-54.
Gaudant J., Cavallo O. & Bonelli E. (2015) - Découverte d'un spécimen d'*Argyropelecus logearti* Arambourg (Poisson téléostéen, Sternoptychidae) dans le Messinien préévaporitique du Tanaro (Verduno, Piémont). *Rivista Piemontese di Storia Naturale*, 36: 23-31.
Goloboff P.A. & Morales M.E. (2023) - TNT version 1.6, with a graphical interface for MacOS and Linux, including new routines in parallel. *Cladistics*, 39: 144-153.
Gordeeva N.V. & Nanova O.G. (2017) - Application of geometric morphometrics for intraspecific variability analysis in mesopelagic fishes of Sternoptychidae and Myctophidae families. *Journal of Ichthyology*, 57: 29-36.
Gregorová R. (1993) - Sur la présence d'*Argyropelecus cosmovicii* Cosmovici et Paucă, 1943 (Poisson téléostéen, Sternoptychidae) dans l'Oligocene des couches à ménilite. *Acta Musei Moraviae*: 39-46.
Haghipour A. & Brants A. (1971) - Eocene remains from the Pabdeh Formation north of Ilam. *Geological Survey of Iran Report*, 19: 81-107.
Harold A.S. (1993) - Phylogenetic relationships of the sternoptychid *Argyropelecus* (Teleostei: Stomiiformes). *Copeia*, 1993: 123-133.
Harold A.S. (1994) - A taxonomic revision of the sternoptychid genus *Polyipnus* (Teleostei: Stomiiformes), with an analysis of phylogenetic relationships. *Bulletin of Marine Science*, 54: 428-534.
Harold A.S. (1998) - Phylogenetic relationships of the Gonostomatidae (Teleostei: Stomiiformes). *Bulletin of Marine Science*, 62: 715-741.
Harold A.S. & Weitzman S.H. (1996) - Interrelationships of stomiiform fishes: 333-353. In: Stiassny M.L.J., Parenti L.R. & Johnson G.D. (Eds.) - Interrelationships of fishes, Academic Press, San Diego.
Hoar W.S., Randall D.J. & Farrell A. (1997) - Deep-Sea Fishes. Academic Press, San Diego, 388 pp.
Hopkins T.L. & Baird R.C. (1973) - Diet of the hatchetfish *Sternoptyx diaphana*. *Marine Biology*, 21: 34-46.
Hopkins T.L. & Baird R.C. (1985) - Feeding ecology of four hatchetfishes (Sternoptychidae) in the eastern Gulf of Mexico. *Bulletin of Marine Science*, 36: 260-277.
Jafarian M.A., Samani P., Bahrami & Pour M. Ghobadi (2000) - Investigation and introduction of some Eocene fossil fishes in Zagros. *University of Isfahan Journal* (*Science*), 13: 181-196.
James G.A. & Wynd J.G. (1965) - Stratigraphic nomenclature of Iranian Oil Consortium Agreement Area. *American Association of Petroleum Geologists Bulletin*, 49: 2182-2245.
Jerzmańska A. (1968) - Ichthyofaune des couches à ménilite. *Acta Palaeontologica Polonica*, 13: 379-488.
Kinzer J. & Schulz K. (1988) - Vertical distribution and feeding patterns of midwater fish in the Central Equatorial Atlantic II. Sternoptychidae. *Marine Biology*, 99(2): 261-269.
Landini W. & Menesini E. (1978) - L'ittiofauna plio-pleistocenica della sezione della Vrica (Crotone - Calabria). *Bollettino della Società Paleontologica Italiana*, 17: 143-175.
Landini W. & Menesini E. (1986) - L'ittiofauna della sez. di Stuni e i suoi rapporti con l'ittiofauna plio-pleistocenica della Vrica (Crotone, Calabria). *Bollettino della Società Paleontologica Italiana,* 25: 41-63.
Landini W. & Sorbini L. (1993) - Biogeographic and paleoclimatic relationships of the Middle Pliocene ichthyofauna of the Samoggia Torrent (Bologna, Italy). *Ciéncias da Terra*, 12: 83-89.
Maddison W. & Maddison D. (2008) - Mesquite: A modular

system for evolutionary analysis. Version 3.03. Accessed 15 November 2023. http://mesquiteproject.org.

May Z. (2019) - Evolutionary relationships and evolution of body shape of the deep-sea. Thesis, College of Science and Engineering, St. Cloud State University, Minnesota (USA).

Mensinger A.F. & Case J.F. (1990) - Luminescent properties of deep-sea fish. *Journal of Experimental Marine Biology and Ecology*, 144(1): 1-15.

Mohseni H. & Al-Asam I.S. (2004) - Tempestite deposits on a storm-influenced carbonate ramp: an example from the Pabdeh Formation (Paleogene), Zagros Basin, SW Iran. *Journal of Petroleum Geology*, 27(2): 163-178.

Mohseni H., Behbahani R., Khodabakh S. & Atashmard Z. (2011) - Depositional environments and trace fossil assemblages in the Pabdeh Formation (Paleogene), Zagros Basin, Iran. *Neues Jahrbuch für Geologie und Paläontologie, Abhandlungen*, 262(2): 59-77.

Murris R.J. (1980) - Middle East: stratigraphic evolution and oil habitat. *Bulletins of the American Association of Petroleum Geologists*, 4: 597-618.

Øyvind H. & Harper D.A.T. (2001) - Past: paleontological statistics software package for educaton and data anlysis. *Palaeontologia electronica,* 4.1.

Parr W.J. (1947) - An Australian record of the foraminiferal genus *Hantkenina*. *Proceedings of the Royal Society of Victoria*, 58: 45-47.

Pauca M. (1933) - De nouveaux Poissons fossiles dans l'Oligocene de Piatra Neamt. *Comptes Rendus des Séances de l'Institute Géologique Roumaine*, 19: 4-12.

Payros A., Dinarès-Turell J., Monechi S. Orue-Etxebarria Z., Ortiz S., Apellaniz E. & Martinez-Braceras N. (2015) - The Lutetian/Bartonian transition (middle Eocene) at the Oyambre section (northern Spain): Implicatins for standard chronostratigraphy. *Palaeogeography, Palaeoclimatology, Palaeoecology*, 440: 234-248.

Pilade F., Licata M., Vasiliev I., Fubelli G. & Gennari, R. (2025) - The GEMMA (Geo-EnvironMental multivariate analysis) toolbox: A user-friendly software for multivariate analysis. *Computers & Geosciences*, 199: 105914.

Priede I.G. (2017) - Deep-Sea Fishes: Biology, Diversity, Ecology and Fisheries. Cambridge University Press, Cambridge (UK), 544 pp.

Priem F. (1908) - Poissons fossiles de Perse. *Annales d'Histoire Naturelle, Paléontologie*, 1: 1-25.

Přikryl T. & Bannikov A.F. (2014) - A new species of the Oligocene pomfret fish *Paucaichthys* (Perciformes; Bramidae) from Iran. *Neues Jahrbuch für Geologie und Paläontologie*. *Abhandlungen*, 272 (3): 325-330.

Přikryl T., Brzobohatý R. & Gregorová R. (2016) - Diversity and distribution of fossil codlets (Teleostei, Gadiformes, Bregmacerotidae): review and commentary. *Palaeobiodiversity and Palaeoenvironments*, 96 (1):13-39.

Prokofiev A.M. (2002) - Sternoptychidae (Stomiiformes) in Eocene to Lower Oligocene of Caucasus and Ukrainian Carpathian Mountains. *Journal of Ichthyology*, 42: 19-27.

Prokofiev A.M. (2005) - Systematics and phylogeny of the stomiiform fishes (Neoteleostei: Stomiiformes) from the Paleogene-Neogene of Russia and adjacent regions. *Journal of Ichthyology*, 45: S89-S162.

Prokofiev A.M. (2010) - Two new genera of Oligocene Stomiiformes. *Journal of Ichthyology*, 50: 590-595.

Rohlf F.J. (2003) - TpsRelw, Relative Warps Analysis, version 1.36. Stony Brook: State University of New York.

Rohlf F.J. (2005) - TpsDig, digitize landmarks and outlines, version 2.05. Stony Brook: State University of New York.

Rohlf F.J. & Corti M. (2000) - Use of two-block partial least-squares to study covariation in shape. *Systematic Biology* 49(4):740-753.

Rohlf F.J. & Slice D.E. (1990) - Extensions of the Procrustes method for the optimal superimposition of landmarks. *Systematic Biology* 39(1):40-59.

Sampò M. (1969) - Microfacies and microfossils of the Zagros Area, Southwestern Iran (from pre-Permian to Miocene). E.J. Brill, Leiden, 102 pp.

Schrøder A.E. & Carnevale G. (2023) - The argentiniform *Surlykus longigracilis* gen. et sp. nov., the most abundant fish from the Eocene Fur Formation of Denmark. *Bulletin of the Geological Society of Denmark*, 72: 1-18.

Schrøder A.E. & Carnevale, G. (2025). - The putative lampridiform *Iratusichthys ulrikii* gen. et sp. nov. from the Stolleklint clay unit of the Ølst Formation, Denmark. *Bulletin of the Geological Society of Denmark,* 74: 33-47.

Schrøder A.E., Rasmussen J.A., Møller P.R. & Carnevale G. (2022) - A new beardfish (Teleostei, Polymixiiformes) from the Eocene Fur Formation, Denmark. *Journal of Vertebrate Paleontology*, 42(2): e2142914.

Schrøder A.E., Wielandt D.K.P., Rasmussen J.A., Carnevale G. & Storey M. (2023) - Benchtop micro-X-ray fluorescence (μXRF): An exciting tool for anatomical studies of fossil bony fishes. *Lethaia*, 56: 1-29.

Schultz L.P. (1938) - Review of the fishes of the genera *Polyipnus* and *Argyropelecus* (Family Sternoptychidae), with descriptions of three new species. *Proceedings of the United States National Museum*, 86: 135-155.

Schultz L.P. (1961) - Revision of the marine silver hatchetfishes (family Sternoptychidae). *Proceedings of the United States National Museum*, 112: 587-649.

Schultz L.P. (1964) - Family Sternoptychidae. In: Fishes of the Western North Atlantic: 241-273. Sears Foundation for Marine Research, Yale University, New Haven.

Sorbini L. (1988) - Biogeography and climatology of Pliocene and Messinian fossil fish of Eastern-Central Italy. *Bollettino del Museo Civico di Storia Naturale di Verona*, 14: 1-85.

Tyler J.C (2000) - *Arambourgthurus*, a new genus of hypurostegic surgeonfish (Acanthuridae) from the Oligocene of Iran, with a phylogeny of the Nasinae. *Geodiversitas*, 22: 525-537.

Tyler J.C., Mirzaie M. & Nazemi A. (2006) - New genus and species of basal tetraodontoid pufferfish from the Oligocene of Iran, related to the Zignoichthyidae (Tetraodontiformes). *Bollettino del Museo Civico di Storia Naturale di Verona*, 30: 49-58.

Weitzman S.H. (1974) - Osteology and evolutionary relationships of the Sternoptychidae, with a new classification of stomiatoid families. *Bulletin of the American Museum of Natural History*, 153: 328-478.

Zelditch M.L., Swiderski D.L., Sheets H.D. & Fink W.L. (2004) - Geometric morphometrics for biologists: a primer. Amsterdam: Elsevier Academic Press, 478 pp.